symmetry

MDPI

Article

The Aboodh–Temimi–Ansari Technique for the Time-Fractional Drinfeld–Sokolov–Wilson System: Convergence Analysis and Numerical Validation

Ahmed Hagag [1,*] and Areej Almuneef [2]

[1] Department of Mathematics and Computer Science, Faculty of Biotechnology, Sinai University, Ismailia 41636, Egypt
[2] Department of Mathematical Sciences, College of Science, Princess Nourah Bint Abdulrahman University, P.O. Box 84428, Riyadh 11671, Saudi Arabia
* Correspondence: ahmed.shehata@su.edu.eg

Abstract

The Drinfeld–Sokolov–Wilson (DSW) system originates in the theory of affine Lie algebras and the Korteweg–de Vries hierarchy, so that its integrability reflects an underlying algebraic symmetry that persists in rescaled form under fractionalization, and it also models dispersive shallow-water waves. This work applies the hybrid Aboodh–Temimi–Ansari technique to the time-fractional DSW system under the Caputo derivative, a scheme that requires neither Adomian nor He polynomials. We show that its iterates are exactly the Picard iterates of an equivalent fractional Volterra integral equation. Under a Lipschitz condition on the nonlinear operator, this yields the existence and uniqueness of a local solution by a Banach fixed-point argument, together with explicit bounds on the truncation error. We also show that the dispersive term of the DSW system prevents this condition from holding in the classical spaces of bounded smooth functions, so that the well-posedness of the fractional system itself remains open. Two initial value problems built from known kink and soliton profiles are solved, recovering the exact classical solution when the fractional order equals one. After two corrections, the approximations agree with the exact profiles to several significant figures, with the residual error concentrated where the nonlinear coupling is largest.

Keywords: Aboodh transform; Temimi–Ansari method; fractional calculus; Drinfeld–Sokolov–Wilson (DSW) system; banach fixed point

Check for updates

Academic Editor: Calogero Vetro

Received: 1 September 2026
Revised: 3 October 2026
Accepted: 13 October 2026
Published: 16 October 2026

Copyright: © 2026 by the authors. Licensee MDPI, Basel, Switzerland. This article is an open access article distributed under the terms and conditions of the Creative Commons Attribution (CC BY) license.

1. Introduction

Nonlinear partial differential equations (PDEs) underlie the mathematical description of wave propagation, fluid motion, and diffusion in almost every branch of applied science. Exact closed-form solutions are available only for a limited number of these equations, and even when such solutions exist, they rarely extend to the fractional-order generalizations that are now used to capture memory and hereditary effects absent from classical integer-order models [1]. The Caputo derivative in particular has become the standard operator for this purpose because it accommodates conventional initial conditions and reduces smoothly to the integer-order case, which makes it convenient for the boundary and initial value problems arising in engineering and physics. As analytic solutions of fractional nonlinear PDEs are generally out of reach, research over the last two decades has shifted

toward semi-analytical and iterative techniques that approximate the solution as a rapidly convergent series while avoiding discretization of the domain.

Among the nonlinear systems that have benefited from this shift is the Drinfeld–Sokolov–Wilson (DSW) system, introduced by Drinfel'd and Sokolov and independently by Wilson in the early 1980s in connection with the Korteweg–de Vries hierarchy and affine Lie algebras [2,3]. Beyond its algebraic origin, the DSW system describes the evolution of dispersive shallow-water waves. Its coupled, cubically nonlinear character makes it a demanding test case for any new solution method, and the fractional-order extension of the system, obtained by replacing the classical time derivative with a Caputo operator, introduces the additional difficulty of handling memory effects in a coupled nonlinear setting.

The fractional DSW system was chosen for three reasons. Its integrability rests on an algebraic symmetry, which places it naturally within the study of symmetry and supplies exact solutions against which approximations can be measured. Its dispersive coupling is precisely the feature that makes convergence claims for semi-analytical methods hardest to justify. And although many such methods have been applied to it, none has established that the problem being approximated has a solution. The contributions of the paper are the following: The hybrid Aboodh–Temimi–Ansari technique, denoted $(\mathrm{AT})^2$, is applied to the time-fractional DSW system, to which, to our knowledge, it has not been applied before, and closed-form iterates are derived for two benchmark problems. The $(\mathrm{AT})^2$ iterates are shown to be exactly the Picard iterates of an equivalent fractional Volterra integral equation. Under a Lipschitz condition on the nonlinear operator this yields local existence and uniqueness and an explicit truncation bound, while a local truncation estimate holds for the iterates without any such condition. The obstruction to applying this theory to the DSW system is identified precisely: the third-order dispersive term loses derivatives, so the Lipschitz condition fails in the classical function spaces, and the only estimate that does hold is given explicitly. This locates what a well-posedness theory for the fractional system requires. The iterates are shown to be independent of the choice of Laplace-type transform, and at $\alpha = 1$ they coincide with those of the variational iteration method. Inconsistent data for both benchmark problems in the literature are identified and corrected, and the corrected results are validated against published values and compared with the Adomian decomposition method.

The paper is organised as follows. Section 2 reviews the existing literature and identifies the gap the paper addresses. Section 3 collects the properties of the Caputo derivative and the Aboodh transform used below. Section 4 derives the $(\mathrm{AT})^2$ recursion, and Section 5 develops its convergence theory and identifies the obstruction to applying it to the DSW system. Section 6 applies the scheme to two initial value problems, Section 7 discusses the numerical results, and Section 8 concludes.

2. Literature Review

The DSW system was not proposed as a phenomenological model and then found to be integrable. It arose the other way round. Drinfel'd and Sokolov obtained it from a reduction associated with an affine Kac–Moody algebra, and Wilson derived the same equations from a modified Lax hierarchy [2,3]. Its integrability is a consequence of that algebraic structure rather than a property discovered after the fact, and this is what separates it from the many coupled KdV-type systems it superficially resembles. Hirota, Grammaticos and Ramani examined the soliton structure of the system soon afterwards [4], and the conservation laws of the classical system were later obtained systematically by the multiplier approach [5].

Extending symmetry analysis to fractional equations is not automatic, since the Caputo and Riemann–Liouville operators do not obey the Leibniz rule that the classical prolon-

gation formulas rely on. The standard route uses the Erdélyi–Kober operators to reduce an invariant fractional PDE to a fractional ODE, and it has been applied to a number of equations in the KdV family: the fifth-order KdV equation [6], the modified KdV equation [7], the biological population model [8], and more recently the stochastic potential-KdV equation [9]. Coupled systems have received less attention, although symmetry reductions with conservation laws have been obtained for fractional coupled Hirota equations [10] and, most relevantly here, for the time-fractional Drinfeld–Sokolov–Satsuma–Hirota system [11]. Lie analysis of this kind continues to be applied to nonlinear models across physics [12–14].

For the fractional DSW system itself no such classification appears to have been carried out, and we do not attempt one here. Two elementary symmetries are nevertheless available, and both are used below. The system is unchanged when the second unknown changes sign, since the first equation is quadratic in that unknown while every term of the second is linear in it. It also admits a scaling invariance in which the fractional order enters only through the exponent governing the temporal variable, the classical scaling being recovered when that order equals one. The family of initial data used in Section 6.2 (Example 2) of Section 6 is an orbit of this scaling, which accounts for the regular dependence of the computed corrections on the wave-speed parameter reported in Section 7. A full Lie classification of the fractional system remains open, and we record it here as such.

One strand of the literature looks for exact travelling waves by substituting a prescribed functional form into the system and solving the resulting algebraic constraints. Exponential and modified exponential function methods were applied to the Drinfel'd–Sokolov system in this way [15], followed by Bäcklund transformations with a Riccati trial function [16] and by several expansion schemes producing soliton and rational solutions [17,18]. A recent study of the fractional-order system in this spirit also carries out a modulation instability analysis, which gives some information about which of the constructed waves are physically relevant [19].

These methods reveal the wave structures the system supports, and the solutions they produce are exact. Their limitation is structural. The form of the solution is assumed at the outset, so the method returns nothing when the initial data fall outside the assumed family, and it says nothing about whether a solution exists for such data.

The second strand pairs an integral transform with an iterative or series construction. The transform removes the fractional derivative, and some auxiliary device resolves the nonlinearity. The devices in use fall into three groups, and each carries a characteristic cost.

Decomposition-based schemes expand the nonlinear term into Adomian or He polynomials [20,21]. Applied to the DSW system through the natural and Sumudu transforms [22–24] and through homotopy perturbation [25,26], they are straightforward to set up, but the number of terms in the polynomials grows combinatorially with the order. Homotopy-based variants [27,28], also applied to the closely related sixth-order Drinfeld–Sokolov–Satsuma–Hirota equation [29] and to coupled fractional reaction–diffusion systems, for which a uniqueness theorem and truncation-error bounds were also derived [30], avoid the polynomials at the price of a convergence-control parameter, which has no a priori determination and is fixed in practice by inspecting an $\hbar$-curve [31]. Residual power series schemes [32,33] need neither, but require the Caputo derivative of the residual to be recomputed at every order; the Aboodh-based versions applied to this system inherit that cost [34].

A parallel line of work has examined the DSW system under non-singular and fractal–fractional operators [35–37], and a quadrature-based numerical treatment has appeared recently [38]. Comparable schemes for related fractional systems in shallow-water and wave settings continue to be developed [39–41], and a survey of the broader family of

semi-analytical methods is available in [42]. The time-fractional DSW system has also been studied analytically in this journal [43].

For a system in which each equation involves the spatial derivatives of both unknowns, these costs grow quickly with the order of approximation for general nonlinearities, although for quadratic terms such as those of the DSW system, the Adomian polynomials reduce to simple Cauchy products. Avoiding these devices is what motivates the pairing used here; Section 7 shows that, for the DSW system, its accuracy is comparable to that of ADM. The Aboodh transform reduces a Caputo derivative to a polynomial factor in the transform variable [44–46], but on its own it cannot invert a nonlinear equation, which is why it is normally combined with one of the devices above [34]. The iterative technique of Temimi and Ansari supplies the missing ingredient by a different device: it evaluates the nonlinear operator directly on the previous iterate, so that neither auxiliary polynomials nor an embedding parameter are needed [47,48]. In fractional form it has been applied, with a convergence analysis, to the KdV–Burgers and Benjamin–Bona–Mahony–Burgers equations [49], and the combination with the Aboodh transform was formalised for systems of fractional PDEs in [50] and applied to the fractional modified Camassa–Holm and Degasperis–Procesi equations [51]. As Remark 3 shows, the resulting iterates do not depend on the particular Laplace-type transform used.

The gap in the literature is not computational. The semi-analytical treatments of the fractional DSW system establish convergence of the series they construct, and in some cases a truncation estimate, without first establishing that the initial value problem has a solution. An estimate of this kind bounds the distance between successive partial sums. It does not bound the distance between the approximation and a solution, because no solution has been shown to exist.

The contrast with the classical system is instructive. Well-posedness for the classical DSW system was settled only recently, by Christov, Hakkaev, Oh and Stefanov, who proved local well-posedness in $L^2 \times L^2$ on the periodic background, extended it to global solutions using the conservation law, and analysed the spectral stability of the periodic waves [52]. That this required a dedicated analysis is itself informative. The third-order dispersive term costs three spatial derivatives and the nonlinear terms cost one more, so that no simple fixed-point argument in spaces of smooth functions closes. For other coupled fractional systems the question has been settled by a different route: for the time-fractional Navier–Stokes equations, local and global existence and uniqueness of mild solutions were obtained by expressing the solution through operators of Mittag–Leffler type [53]. There, however, the linear part is dissipative and supplies the smoothing that the fixed-point argument requires, whereas the linear part of the DSW system is dispersive and supplies none. Nothing comparable is available for the fractional DSW system.

The present paper does not close this gap, but it locates it precisely. Recognising the $(\mathrm{AT})^2$ recursion as the Picard iteration of a fractional Volterra integral equation shows that existence, uniqueness, and rigorous error bounds all follow from a single Lipschitz condition on the nonlinear operator. Section 5 proves this, and then shows that the condition fails for the DSW operator in the spaces C_b^k for exactly the reason just described. What a well-posedness theory of the fractional system still requires is a setting in which the dispersive term is controlled, and we indicate a natural candidate. The scheme is then applied to two initial value problems built from known kink and soliton profiles, and reduces to the exact classical solution when the fractional order equals one.

3. Preliminaries to Fractional Calculus

This section collects the definitions and operational properties of the Caputo derivative and the Aboodh transform that are used throughout the paper.

3.1. Fractional Operators in the Caputo Sense

Definition 1. *Let $\alpha > 0$. The Riemann–Liouville fractional integral of order α of a function $\Upsilon(\theta,\cdot) \in L^1(0,T)$ is defined by [1]*

$$I_\eta^\alpha \Upsilon(\theta,\eta) = \frac{1}{\Gamma(\alpha)} \int_0^\eta (\eta-\mu)^{\alpha-1} \Upsilon(\theta,\mu)\, d\mu, \qquad \eta > 0. \tag{1}$$

Definition 2. *Let $\sigma - 1 < \alpha \le \sigma$ with $\sigma \in \mathbb{N}$, and let $\Upsilon(\theta,\cdot) \in AC^\sigma[0,T]$. The Caputo fractional derivative of order α with respect to η is defined by [1]*

$$D_\eta^\alpha \Upsilon(\theta,\eta) = \frac{1}{\Gamma(\sigma-\alpha)} \int_0^\eta (\eta-\mu)^{\sigma-\alpha-1} \frac{\partial^\sigma \Upsilon(\theta,\mu)}{\partial \mu^\sigma}\, d\mu, \tag{2}$$

which reduces to the classical derivative $\frac{\partial^\sigma \Upsilon}{\partial \eta^\sigma}$ when $\alpha = \sigma$.

Remark 1. *The Caputo derivative is adopted here rather than the Riemann–Liouville derivative because (2) admits initial conditions expressed in terms of integer-order derivatives of Υ at $\eta = 0$, which is the form in which the initial data of the fractional Drinfeld–Sokolov–Wilson system are naturally prescribed, and because $D_\eta^\alpha c = 0$ for every constant c.*

Proposition 1. *Let $0 < \alpha \le 1$ and let $\Upsilon(\theta,\cdot) \in AC[0,T]$. Then*

$$I_\eta^\alpha D_\eta^\alpha \Upsilon(\theta,\eta) = \Upsilon(\theta,\eta) - \Upsilon(\theta,0), \qquad D_\eta^\alpha I_\eta^\alpha \Upsilon(\theta,\eta) = \Upsilon(\theta,\eta). \tag{3}$$

Moreover, for every $\beta > -1$,

$$I_\eta^\alpha \eta^\beta = \frac{\Gamma(\beta+1)}{\Gamma(\beta+\alpha+1)} \eta^{\beta+\alpha}. \tag{4}$$

Proof. See [1,54]. □

3.2. The Aboodh Transform

Definition 3. *A function $\Upsilon(\eta)$ is said to be of exponential order if there exist constants $M, k_1, k_2 > 0$ such that $|\Upsilon(\eta)| < Me^{k_j \eta}$ for $\eta \in (-1)^j \times [0,\infty)$, $j = 1,2$; we denote by G the set of all such functions. For $\Upsilon \in G$, the Aboodh transform $\varkappa$ is defined by [44,46]*

$$\varkappa[\Upsilon(\eta)](s) = \lambda(s) = \frac{1}{s} \int_0^\infty e^{-s\eta} \Upsilon(\eta)\, d\eta, \qquad k_1 \le s \le k_2. \tag{5}$$

For a function of two variables the transform is taken in η, with θ acting as a parameter, and we write $\varkappa[\Upsilon(\theta,\eta)](s) = \lambda(\theta,s)$.

Definition 4. *The inverse Aboodh transform is given by the Bromwich-type integral [46]*

$$\varkappa^{-1}[\lambda(s)] = \Upsilon(\eta) = \frac{1}{2\pi i} \int_{a-i\infty}^{a+i\infty} s\, e^{s\eta} \lambda(s)\, ds, \tag{6}$$

where a is chosen so that the contour lies to the right of all singularities of $s\,\lambda(s)$.

Lemma 1 ([44,46])**.** *Let $\Upsilon_1, \Upsilon_2 \in G$ have Aboodh transforms $\lambda_1(s)$ and $\lambda_2(s)$, respectively. Then for all $\delta_1, \delta_2 \in \mathbb{R}$,*

$$\varkappa[\delta_1 \Upsilon_1(\eta) \pm \delta_2 \Upsilon_2(\eta)] = \delta_1 \lambda_1(s) \pm \delta_2 \lambda_2(s). \tag{7}$$

The same identity holds for $\varkappa^{-1}$.

Lemma 2 ([45]). *Let* $\mathrm{Y} \in G$ *with exponential order* k_1*, and let* $s > k_1$*. Denote by*

$$\mathcal{L}[\mathrm{Y}(\eta)](s) = F(s) = \int_0^\infty e^{-s\eta}\mathrm{Y}(\eta)\, d\eta \tag{8}$$

the Laplace transform of Y*. Then both (5) and* $F(s)$ *converge absolutely for every* $s > k_1$*, and*

$$\lambda(s) = \frac{F(s)}{s}, \qquad \textit{equivalently} \qquad F(s) = s\,\lambda(s). \tag{9}$$

Consequently $\varkappa$ *is injective on* G*, and*

$$\varkappa^{-1}[\lambda(s)] = \mathcal{L}^{-1}[s\,\lambda(s)], \qquad \mathcal{L}^{-1}[F(s)] = \varkappa^{-1}\left[\frac{F(s)}{s}\right]. \tag{10}$$

Proof. Since $\mathrm{Y} \in G$, there are $M > 0$ and $k_1 > 0$ with $|\mathrm{Y}(\eta)| \le Me^{k_1\eta}$ for all $\eta \ge 0$. Hence, for $s > k_1$,

$$\int_0^\infty |e^{-s\eta}\mathrm{Y}(\eta)|d\eta \le M\int_0^\infty e^{-(s-k_1)\eta}d\eta = \frac{M}{s-k_1} < \infty, \tag{11}$$

so $F(s)$ converges absolutely on (k_1, ∞), and so does (5), which differs from it only by the factor s^{-1}. Comparing the two definitions termwise gives $\lambda(s) = s^{-1}\mathcal{L}[\mathrm{Y}](s) = F(s)/s$, which is (9). If $\lambda \equiv 0$ on (k_1, ∞) then $F \equiv 0$ there, and the injectivity of the Laplace transform on G forces $\mathrm{Y} = 0$ almost everywhere; thus $\varkappa$ is injective. Relations (10) follow by applying $\varkappa^{-1}$ and $\mathcal{L}^{-1}$ to (9). □

Corollary 1. *For every* $\beta > -1$*,* $a \in \mathbb{R}$ *and* $s > 0$*,*

$$\varkappa\left[\eta^\beta\right] = \frac{\Gamma(\beta+1)}{s^{\beta+2}}, \qquad \varkappa[e^{a\eta}] = \frac{1}{s(s-a)}, \qquad \varkappa[\sin(a\eta)] = \frac{a}{s(s^2+a^2)}, \qquad \varkappa[\cos(a\eta)] = \frac{1}{s^2+a^2}. \tag{12}$$

In particular $\varkappa[1] = s^{-2}$ *and* $\varkappa[\eta] = s^{-3}$*. These and further elementary pairs are collected in Table 1.*

Proof. Immediate from Lemma 2 together with the classical Laplace transforms $\mathcal{L}\left[\eta^\beta\right] = \Gamma(\beta+1)s^{-\beta-1}$, $\mathcal{L}[e^{a\eta}] = (s-a)^{-1}$, $\mathcal{L}[\sin(a\eta)] = a\left(s^2+a^2\right)^{-1}$ and $\mathcal{L}[\cos(a\eta)] = s\left(s^2+a^2\right)^{-1}$, each divided by s. □

Table 1. Aboodh transform of some elementary functions.

$\mathbf{Y(\eta)}$	$\varkappa[\mathbf{Y}(\boldsymbol{\eta})] = \boldsymbol{\lambda(s)}$
1	$\frac{1}{s^2}$
η	$\frac{1}{s^3}$
$\eta^\beta,\ \beta > -1$	$\frac{\Gamma(\beta+1)}{s^{\beta+2}}$
$e^{a\eta}$	$\frac{1}{s(s-a)}$
$\sin(a\eta)$	$\frac{a}{s(s^2+a^2)}$
$\cos(a\eta)$	$\frac{1}{s^2+a^2}$
$\eta^{\alpha-1}E_{\alpha,\alpha}(a\eta^\alpha)$	$\frac{1}{s^2(s^\alpha-a)}$

Remark 2. *In the last row $E_{\alpha,\gamma}(z) = \sum_{m=0}^{\infty} z^m/\Gamma(\alpha m + \gamma)$ denotes the two-parameter Mittag–Leffler function, which plays for linear fractional equations the role that the exponential plays in the integer-order case [1]. Every entry of Table 1 is obtained from the corresponding Laplace pair through Lemma 2; the inverse pairs follow by reading the table from right to left, which is legitimate by the injectivity established in the same theorem.*

3.3. Operational Properties for Fractional Operators

Theorem 1. *Let $\sigma - 1 < \alpha \le \sigma$, $\sigma \in \mathbb{N}$, and suppose that $\Upsilon(\theta, \cdot)$ and its derivatives up to order $\sigma - 1$ belong to G. Then the Aboodh transform of the Caputo derivative (2) is [45]*

$$\varkappa\Big[D_\eta^\alpha \Upsilon(\theta,\eta)\Big](s) = s^\alpha \lambda(\theta,s) - \sum_{l=0}^{\sigma-1} \frac{\Upsilon^{(l)}(\theta,0)}{s^{2-\alpha+l}}, \tag{13}$$

where $\Upsilon^{(l)}(\theta,0) = \partial^l \Upsilon(\theta,\eta)/\partial\eta^l\big|_{\eta=0}$. In particular, for $0 < \alpha \le 1$,

$$\varkappa\Big[D_\eta^\alpha \Upsilon(\theta,\eta)\Big](s) = s^\alpha \lambda(\theta,s) - \frac{\Upsilon(\theta,0)}{s^{2-\alpha}}. \tag{14}$$

Proof. The Laplace transform of the Caputo derivative is

$$\mathcal{L}\Big[D_\eta^\alpha \Upsilon\Big](s) = s^\alpha F(\theta,s) - \sum_{l=0}^{\sigma-1} s^{\alpha-l-1}\Upsilon^{(l)}(\theta,0) \tag{15}$$

[1]. Dividing by s and substituting $F(\theta,s) = s\,\lambda(\theta,s)$ from (9) gives

$$\varkappa\Big[D_\eta^\alpha \Upsilon\Big](s) = s^{\alpha-1}\cdot s\,\lambda(\theta,s) - \sum_{l=0}^{\sigma-1} s^{\alpha-l-2}\Upsilon^{(l)}(\theta,0) = s^\alpha\lambda(\theta,s) - \sum_{l=0}^{\sigma-1}\frac{\Upsilon^{(l)}(\theta,0)}{s^{2-\alpha+l}}, \tag{16}$$

which is (13). Setting $\sigma = 1$ yields (14). □

Proposition 2. *Let $\alpha > 0$ and let $g(\theta,\cdot) \in G$ with $\varkappa[g] = \lambda_g$. Then*

$$\varkappa\Big[I_\eta^\alpha g(\theta,\eta)\Big](s) = \frac{\lambda_g(\theta,s)}{s^\alpha}, \qquad \textit{equivalently} \qquad \varkappa^{-1}\left[\frac{1}{s^\alpha}\varkappa[g(\theta,\eta)]\right] = I_\eta^\alpha g(\theta,\eta). \tag{17}$$

Proof. By (1), $I_\eta^\alpha g$ is the convolution of g with $\eta^{\alpha-1}/\Gamma(\alpha)$, so the convolution theorem for the Laplace transform gives $\mathcal{L}\Big[I_\eta^\alpha g\Big] = s^{-\alpha}\mathcal{L}[g]$. Dividing by s and applying (9) to both sides yields the first identity in (17); the second follows by applying $\varkappa^{-1}$, which is well defined by Lemma 2. □

Remark 3. *The identity of Proposition 2 does not depend on the Aboodh transform. The Laplace transform satisfies $\mathcal{L}\Big[I_\eta^\alpha g\Big] = s^{-\alpha}\mathcal{L}[g]$ [1], so the composite operator $\mathcal{L}^{-1}[s^{-\alpha}\mathcal{L}[\,\cdot\,]]$ is also the Riemann–Liouville integral I_η^α, and the same holds for the other Laplace-type transforms used in this context, such as the Sumudu and natural transforms. Consequently the Temimi–Ansari recursion built on the Laplace transform produces exactly the same iterates as the $(AT)^2$ recursion, and a numerical comparison between the two would give identical values. The choice of the Aboodh transform is a matter of convenience. For this reason the comparison in Section 7 is made with a method that resolves the nonlinearity differently, the Adomian decomposition method, which by the same argument coincides with its Laplace-transform variant.*

Remark 4. *Proposition 2 is the identity on which the whole construction rests: it shows that the composite operator $\varkappa^{-1}[s^{-\alpha}\varkappa[\,\cdot\,]]$, which appears at every step of the $(\mathrm{AT})^2$ recursion derived in*

Section 4, is nothing but the Riemann–Liouville fractional integral I_η^α. This is what allows the iterative scheme to be recast as a fractional Volterra integral equation and analysed by fixed-point methods in Section 5.

4. Fundamental Steps for the $(AT)^2$

This section outlines the fundamental steps of the $(AT)^2$ technique for constructing the general solution of fractional partial differential equations (FPDEs), where the fractional derivative is understood in the Caputo sense. Consider the nonlinear equation

$$D_\eta^\alpha \mathrm{Y}(\theta,\eta) + M\mathrm{Y}(\theta,\eta) = h(\theta,\eta), \tag{18}$$

where $D_\eta^\alpha = \frac{\partial^\alpha}{\partial \eta^\alpha}$ denotes the Caputo derivative operator, M represents the general linear and nonlinear differential operators, and h is a known continuous function, subject to the initial condition

$$\mathrm{Y}(\theta,0) = h(\theta,0). \tag{19}$$

Applying the AT to Equation (18) and subsequently the inverse AT yields

$$\mathrm{Y}(\theta,\eta) = h(\theta,0) + \varkappa^{-1}\left[\frac{1}{s^\alpha}\varkappa[h(\theta,\eta)]\right] - \varkappa^{-1}\left[\frac{1}{s^\alpha}[\varkappa[M\mathrm{Y}(\theta,\eta)]]\right]. \tag{20}$$

The solution of Equation (18) is then obtained through the iterative scheme of the TAM methodology. The first approximation is given by

$$\mathrm{Y}_0(\theta,\eta) \quad = \quad h(\theta,0) + \varkappa^{-1}\left[\frac{1}{s^\alpha}\varkappa[h(\theta,\eta)]\right]. \tag{21}$$

The subsequent iterations, for $\sigma \geq 1$, are computed in an analogous manner, with each successive iterate providing a refined approximation to the solution of the problem. Proceeding in this way, we obtain

$$\mathrm{Y}_\sigma(\theta,\eta) = \mathrm{Y}_0(\theta,\eta) - \varkappa^{-1}\left[\frac{1}{s^\alpha}[\varkappa[M\mathrm{Y}_{\sigma-1}(\theta,\eta)]]\right]. \tag{22}$$

As $\sigma \to \infty$, the sequence $\mathrm{Y}_\sigma(\theta,\eta)$ converges to the exact solution of Equation (18).

5. Convergence and Error Analysis

The preceding section derived the $(\mathrm{AT})^2$ recursion (22) for the abstract fractional Equation (18). Before applying the scheme to the fractional DSW system in Section 6, we examine here under which conditions the iterates converge to a solution, and how fast the truncation error decays with the number of iterations. The analysis is carried out for the abstract Equation (18) under an explicit Lipschitz condition, Assumption 2 below; the coupled system (43), (52) fits this framework with Y replaced by the pair $U = (\mathrm{Y}, \Phi)$. Whether the DSW nonlinearity satisfies that condition is a separate question, taken up in Remark 6; in the classical function spaces the answer is that it does not.

5.1. Functional Setting

Let $\Omega \subseteq \mathbb{R}$ denote the spatial domain and, for $T > 0$, set $Q_T = \Omega \times [0,T]$. Let X be a Banach space of real functions on Ω. For the coupled unknown $U = (\mathrm{Y}, \Phi)$ we work in the product space $\mathcal{X} = X \times X$, $\|U\|_{\mathcal{X}} = \|\mathrm{Y}\|_X + \|\Phi\|_X$, and, for fixed $T > 0$, in $\mathcal{Y}_T = C([0,T];\mathcal{X})$ with the sup norm $\|U\|_{\mathcal{Y}_T} = \sup_{\eta\in[0,T]}\|U(\cdot,\eta)\|_{\mathcal{X}}$, which is again a

Banach space. The choice of X is dictated by the nonlinearity. For the DSW system the obvious candidates are the spaces

$$C_b^k(\Omega) = \Big\{ \varphi \in C^k(\Omega) : \ \partial_\theta^j \varphi \in C_b(\Omega), \ j = 0, \dots, k \Big\}, \qquad \|\varphi\|_{C_b^k} = \sum_{j=0}^{k} \Big\| \partial_\theta^j \varphi \Big\|_\infty, \tag{23}$$

with $k \geq 3$, since the second equation of (43) involves $\Phi_{\theta\theta\theta}$. We show in Remark 6 that none of them is adequate for the full DSW operator, and for this reason the results below are stated for a general X.

Assumption 1. *The initial data satisfy $U(\cdot, 0) = (\Upsilon(\cdot, 0), \Phi(\cdot, 0)) \in \mathcal{X}$, and the source term satisfies $h \in C([0, T]; \mathcal{X})$; for the DSW system $h \equiv 0$.*

For the initial data of Examples 1 and 2 the relevant regularity is not in question: the profiles $\tanh^2$, sech and sech^2 are $C^\infty(\mathbb{R})$ with all derivatives bounded on $\mathbb{R}$, so they belong to $C_b^k(\mathbb{R})$ for every k.

5.2. An Equivalent Fractional Volterra Formulation

The next lemma shows that the transform pair used in the $(\mathrm{AT})^2$ scheme is, in fact, a disguised Riemann–Liouville fractional integral, which allows the convergence theory of fractional Volterra equations to be brought to bear on the recursion (22).

Lemma 3. *For every $\alpha > 0$ and every $g(\theta, \cdot)$ admitting an Aboodh transform,*

$$\varkappa^{-1}\left[\frac{1}{s^\alpha} \varkappa[g(\theta, \eta)] \right] = \frac{1}{\Gamma(\alpha)} \int_0^\eta (\eta - \mu)^{\alpha - 1} g(\theta, \mu) \, d\mu =: I_\eta^\alpha g(\theta, \eta), \tag{24}$$

i.e., the composite operator $\varkappa^{-1}[s^{-\alpha} \varkappa[\,\cdot\,]]$ coincides with the Riemann–Liouville fractional integral of order α in η.

Proof. This is Proposition 2, restated in the form used below. □

By Lemma 3 and the semigroup property $I_\eta^\alpha D_\eta^\alpha \Upsilon(\theta, \eta) = \Upsilon(\theta, \eta) - \Upsilon(\theta, 0)$ for $0 < \alpha \leq 1$ [1], Equation (18) together with its initial condition is equivalent to the nonlinear Volterra integral equation

$$\Upsilon(\theta, \eta) = \Upsilon_0(\theta, \eta) - I_\eta^\alpha [M\Upsilon](\theta, \eta), \qquad \Upsilon_0(\theta, \eta) := \Upsilon(\theta, 0) + I_\eta^\alpha h(\theta, \eta), \tag{25}$$

which matches exactly the initial approximation used to start the $(\mathrm{AT})^2$ recursion. Defining the operator

$$(\mathcal{T}\Upsilon)(\theta, \eta) := \Upsilon_0(\theta, \eta) - I_\eta^\alpha [M\Upsilon](\theta, \eta), \tag{26}$$

(25) reads $\Upsilon = \mathcal{T}\Upsilon$, i.e., the exact solution is a fixed point of $\mathcal{T}$, while by Lemma 3 the recursion (22) reads exactly $\Upsilon_\sigma = \mathcal{T}\Upsilon_{\sigma - 1}$: the $(\mathrm{AT})^2$ iterates are the Picard iterates of $\mathcal{T}$ starting from Υ_0. For the coupled DSW system this reformulation holds componentwise with $U = (\Upsilon, \Phi)$, $U_0 = (\Upsilon(\theta, 0), \Phi(\theta, 0))$, and vector-valued operator

$$\mathcal{M}(U) = (M_1(U), M_2(U)), \qquad M_1(U) = 3\Phi\Phi_\theta, \quad M_2(U) = 2\Phi_{\theta\theta\theta} + 2\Upsilon\Phi_\theta + \Upsilon_\theta\Phi. \tag{27}$$

5.3. Existence and Uniqueness

The derivation of the recursion (22) presupposes that (25) is solvable. We now show that it is, and that the iterates converge to its solution, whenever the nonlinear operator satisfies the following condition.

Assumption 2. *The operator $\mathcal{M}$ maps $\mathcal{X}$ into itself and is Lipschitz on bounded sets: for every $R > 0$ there is $L(R) > 0$ such that*

$$\|\mathcal{M}(U) - \mathcal{M}(V)\|_{\mathcal{X}} \le L(R)\|U - V\|_{\mathcal{X}} \qquad \text{whenever } \|U\|_{\mathcal{X}}, \|V\|_{\mathcal{X}} \le R. \tag{28}$$

Throughout the rest of this section we fix $r > 0$ and set

$$R := \sup_{\eta\in[0,T]} \|U_0(\cdot,\eta)\|_{\mathcal{X}} + r, \qquad L := L(R), \qquad K := \sup_{\eta\in[0,T]} \|\mathcal{M}(U_0(\cdot,\eta))\|_{\mathcal{X}}, \tag{29}$$

all of which are finite by Assumptions 1 and 2, since U_0 is continuous from $[0, T]$ into $\mathcal{X}$ and $\mathcal{M}$ is continuous on $\mathcal{X}$.

Theorem 2. *Let Assumptions 1 and 2 hold. Then there exists $T_0 \in (0, T]$ such that the Volterra Equation (25), equivalently the initial value problem (18), has a unique solution $U \in C([0, T_0]; \mathcal{X})$.*

Proof. Choose $T_0 \in (0, T]$ so small that

$$\frac{T_0^\alpha}{\Gamma(\alpha+1)}(K + Lr) \le r \qquad \text{and} \qquad q := \frac{LT_0^\alpha}{\Gamma(\alpha+1)} < 1. \tag{30}$$

On $\mathcal{Y}_{T_0}$ consider the closed ball $\overline{B}_r(U_0) = \left\{V \in \mathcal{Y}_{T_0} : \|V - U_0\|_{\mathcal{Y}_{T_0}} \le r\right\}$. Every V in it satisfies $\|V(\cdot,\eta)\|_{\mathcal{X}} \le R$, so by (28) and (29), $\|\mathcal{M}(V(\cdot,\eta))\|_{\mathcal{X}} \le K + Lr$ for every $\eta \in [0, T_0]$. Since $\left\|I_\eta^\alpha f\right\|_{\mathcal{Y}_{T_0}} \le \frac{T_0^\alpha}{\Gamma(\alpha+1)}\|f\|_{\mathcal{Y}_{T_0}}$, it follows from (26) that

$$\|\mathcal{T}V - U_0\|_{\mathcal{Y}_{T_0}} \le \frac{T_0^\alpha}{\Gamma(\alpha+1)}(K + Lr) \le r, \tag{31}$$

so $\mathcal{T}$ maps $\overline{B}_r(U_0)$ into itself; $\mathcal{T}V$ is continuous in η because $\mathcal{M}$ is continuous on $\mathcal{X}$ and I_η^α maps $C([0, T_0]; \mathcal{X})$ into itself. For $V, W \in \overline{B}_r(U_0)$, (28) gives

$$\|\mathcal{T}V - \mathcal{T}W\|_{\mathcal{Y}_{T_0}} \le \frac{T_0^\alpha}{\Gamma(\alpha+1)}L\|V - W\|_{\mathcal{Y}_{T_0}} = q\|V - W\|_{\mathcal{Y}_{T_0}}, \tag{32}$$

so $\mathcal{T}$ is a contraction on the complete metric space $\overline{B}_r(U_0)$. By the Banach fixed-point theorem [54], $\mathcal{T}$ has a unique fixed point $U \in \overline{B}_r(U_0)$. For uniqueness in the whole of $\mathcal{Y}_{T_0}$, let U and V be any two solutions of (25) on $[0, T_0]$. Being continuous on a compact interval, both are bounded in $\mathcal{Y}_{T_0}$, say by R', and $w(\eta) := \|U(\cdot,\eta) - V(\cdot,\eta)\|_{\mathcal{X}}$ satisfies $w(\eta) \le L(R')\, I_\eta^\alpha w(\eta)$ by (28). The generalized Gronwall inequality for Volterra equations with a weakly singular kernel [55] then forces $w \equiv 0$. □

Remark 5. *Theorem 2 is local in time, and T_0 depends on the data through K, r and L. If (28) holds globally, with a constant independent of R, the restriction can be removed: the standard weighted-norm argument [54], or the Gronwall inequality of [55], then gives existence and uniqueness on every interval $[0, T]$. Under the local condition Assumption 2 no such extension is available without an a priori bound on the solution, which we do not have. The existence interval guaranteed by the theorem should therefore not be identified with the time range of the numerical experiments in Section 7.*

Remark 6. *The results of this section apply to the fractional DSW system only if the operator (27) satisfies Assumption 2 for some choice of X, and in the spaces $C_b^k(\Omega)$ of (23) it does not. The obstruction is the dispersive term $2\Phi_{\theta\theta\theta}$ in M_2, which maps $C_b^k(\Omega)$ into $C_b^{k-3}(\Omega)$ but not into $C_b^k(\Omega)$. Hence $\mathcal{M}$ does not map $C_b^k \times C_b^k$ into itself for any k, and cannot be Lipschitz there. The quadratic terms $3\Phi\Phi_\theta$, $2\Upsilon\Phi_\theta$ and $\Upsilon_\theta\Phi$ lose one derivative each, so the same obstruction would*

persist, in a weaker form, even without the dispersive term. What does hold is a Lipschitz bound with a loss of derivatives: estimating the linear term and the three products separately, using $\|fg\|_\infty \le \|f\|_\infty \|g\|_\infty$*, one finds*

$$\|\mathcal{M}(U) - \mathcal{M}(V)\|_{C_b \times C_b} \le (2 + 6R)\|U - V\|_{C_b^3 \times C_b^3} \qquad \text{whenever } \|U\|_{C_b^3 \times C_b^3}, \|V\|_{C_b^3 \times C_b^3} \le R. \tag{33}$$

This is precisely the kind of estimate a fixed-point argument cannot use, since $\mathcal{T}$ *must return to the space it starts from. The loss of derivatives is intrinsic to dispersive systems of KdV type, and it is the reason the well-posedness of the classical DSW system required the substantially more delicate analysis of [52]. We therefore do not claim existence or uniqueness for the fractional DSW system: Theorems 2–4 hold for (18) whenever Assumption 2 holds, and establishing Assumption 2, or a substitute for it, for the fractional DSW system remains open. A natural route is a mild formulation in which the dispersive term is treated through its solution operator rather than as part of* $\mathcal{M}$*. After Fourier transformation in* θ *the linear part of the second equation,* $D_\eta^\alpha \Phi = -2\Phi_{\theta\theta\theta}$*, becomes* $D_\eta^\alpha \hat{\Phi} = 2ik^3 \hat{\Phi}$*, with solution* $E_\alpha\left(2ik^3 \eta^\alpha\right)\hat{\Phi}(k, 0)$*, and the Mittag–Leffler function* E_α *is bounded on the imaginary axis for* $0 < \alpha \le 1$ *[1]. The fixed-point problem would then involve only the lower-order nonlinear terms, which still lose one derivative, and closing it would require exploiting the smoothing properties of the associated solution operators, as is done for the time-fractional Navier–Stokes equations [53], where the dissipative linear part makes this possible. We do not pursue this here.*

5.4. Convergence of the $(AT)^2$ Iterates

Theorem 3. *Under the hypotheses of Theorem 2, the sequence* $\{U_\sigma\}_{\sigma \ge 0}$ *generated by (22) remains in* $\overline{B}_r(U_0)$ *for every* σ *and converges in* $\mathcal{Y}_{T_0}$ *to the unique solution* U *of (25), with the geometric error bound*

$$\|U - U_\sigma\|_{\mathcal{Y}_{T_0}} \le \frac{q^\sigma}{1 - q}\|U_1 - U_0\|_{\mathcal{Y}_{T_0}}, \qquad \sigma \ge 0, \tag{34}$$

where $q = \frac{LT_0^\alpha}{\Gamma(\alpha+1)} < 1$ *is the contraction ratio of (32).*

Proof. Since $U_\sigma = \mathcal{T}U_{\sigma-1}$ and $\mathcal{T} : \overline{B}_r(U_0) \to \overline{B}_r(U_0)$ by the proof of Theorem 2, induction on σ shows $U_\sigma \in \overline{B}_r(U_0)$ for every $\sigma \ge 0$. Because $\mathcal{T}$ is a q-contraction there, $\{U_\sigma\}$ is a Picard sequence for the fixed point U, and the classical a priori error estimate for Banach's fixed-point theorem,

$$\|U - U_\sigma\|_{\mathcal{Y}_{T_0}} \le \frac{q^\sigma}{1 - q}\|U_1 - U_0\|_{\mathcal{Y}_{T_0}}, \tag{35}$$

gives (34); convergence $U_\sigma \to U$ follows letting $\sigma \to \infty$ since $q < 1$. □

Corollary 2. *The convergence in Theorem 3 is geometric with ratio* $q = \frac{LT_0^\alpha}{\Gamma(\alpha+1)}$*: each further iteration reduces the error bound by the same factor* q*, independently of* σ*. The rapid stabilization of the partial sums at* $\sigma = 2$ *observed in Examples 1 and 2 is what such a regime would produce, although, by Remark 6, the theorem does not itself apply to the DSW examples.*

5.5. Truncation Error Analysis

We now quantify the error committed when the series is truncated after N iterations, $U_N = \mathcal{T}^N U_0$, as is done in practice.

Theorem 4. *Under the hypotheses of Theorem 2, with* K*,* L*,* r *and* T_0 *as in (29) and (30), for every* $N \ge 0$ *and every* $\eta \in [0, T_0]$*,*

$$\|U(\cdot, \eta) - U_N(\cdot, \eta)\|_{\mathcal{X}} \le (K + Lr)\frac{L^N \eta^{(N+1)\alpha}}{\Gamma((N+1)\alpha + 1)}. \tag{36}$$

In particular $\|U - U_N\|_{\mathcal{Y}_{T_0}} \le (K + Lr)L^N T_0^{(N+1)\alpha}/\Gamma((N+1)\alpha + 1)$, *which tends to zero faster than any geometric sequence as* $N \to \infty$.

Proof. By Theorem 3, U and every iterate U_N lie in $\overline{B}_r(U_0)$, so their values have a norm of at most R and (28) apply with $L = L(R)$. For $N = 0$, $U - U_0 = -I_\eta^\alpha[\mathcal{M}(U)]$ and $\|\mathcal{M}(U(\cdot,\mu))\|_{\mathcal{X}} \le K + Lr$, so $\|U(\cdot,\eta) - U_0(\cdot,\eta)\|_{\mathcal{X}} \le \frac{(K+Lr)\eta^\alpha}{\Gamma(\alpha+1)}$. If the bound holds for $N-1$, then, since $U - U_N = \mathcal{T}U - \mathcal{T}U_{N-1} = -I_\eta^\alpha[\mathcal{M}(U) - \mathcal{M}(U_{N-1})]$,

$$\|U(\cdot,\eta) - U_N(\cdot,\eta)\|_{\mathcal{X}} \le L\, I_\eta^\alpha\left[(K+Lr)\frac{L^{N-1}\mu^{N\alpha}}{\Gamma(N\alpha+1)}\right](\eta) = (K+Lr)\frac{L^N \eta^{(N+1)\alpha}}{\Gamma((N+1)\alpha+1)}, \quad (37)$$

by (4). □

Estimate (36) controls the truncation error both in the number of iterations and in time. The same power structure in η is visible directly in the closed-form corrections of Examples 1 and 2 (for instance $\mathrm{Y}_1 - \mathrm{Y}_0 = O(\eta^\alpha)$, while $\mathrm{Y}_2 - \mathrm{Y}_1$ contains only the higher powers $\eta^{2\alpha}$ and $\eta^{3\alpha}$), and it can be established for the iterates without any hypothesis on existence, using only the algebraic nature of $\mathcal{M}$.

Assumption 3. $\mathcal{M}$ *is a polynomial differential operator in* U *and its* θ*-derivatives, i.e., a finite sum of terms each obtained from* Y, Φ *by* θ*-differentiation and pointwise multiplication. This holds for the DSW operator (27).*

Proposition 3. *Let Assumption 3 hold, let the equation be autonomous,* $h \equiv 0$, *as in (43) and (52), so that* $U_0(\theta,\eta) = U(\theta,0)$ *is independent of* η, *and let the initial data be* C^∞ *in* θ *with all derivatives bounded on* Ω.

(a) For every $\sigma \ge 1$ the correction $\Delta U_\sigma := U_\sigma - U_{\sigma-1}$, together with each of its θ-derivatives, satisfies

$$\Delta U_\sigma(\theta,\eta) = O(\eta^{\sigma\alpha}) \qquad \text{as } \eta \to 0^+, \text{ uniformly in } \theta \in \Omega. \quad (38)$$

(b) If, in addition, (18) has a solution U on some interval $[0, T_1]$ such that U and each of its θ-derivatives is bounded on $\Omega \times [0, T_1]$, then for every $N \ge 0$, uniformly in θ,

$$U(\theta,\eta) - U_N(\theta,\eta) = O\left(\eta^{(N+1)\alpha}\right) \qquad \text{as } \eta \to 0^+. \quad (39)$$

Proof. Each iterate is well defined and smooth in θ with bounded derivatives, since $\mathcal{M}$ involves only θ-differentiation and pointwise products, and I_η^α preserves boundedness on bounded time intervals and commutes with θ-differentiation.

(a) For $\sigma = 1$: since U_0 does not depend on η, neither does $\mathcal{M}(U_0)$, so by Lemma 3 applied to a function constant in η,

$$\Delta U_1(\theta,\eta) = -I_\eta^\alpha[\mathcal{M}(U_0)](\theta,\eta) = -\frac{\eta^\alpha}{\Gamma(\alpha+1)}\mathcal{M}(U_0)(\theta), \quad (40)$$

which is exactly proportional to η^α; this matches the $\frac{\eta^\alpha}{\Gamma(\alpha+1)}$ coefficient in the explicit expressions for Y_1 and Φ_1 in both Examples 1 and 2. Assume inductively that ΔU_j and all its θ-derivatives are $O(\eta^{j\alpha})$ uniformly in θ for $j = 1, \dots, \sigma - 1$. By Assumption 3, $\mathcal{M}$ acts on $U_{\sigma-1}$ and $U_{\sigma-2}$ through finite sums of θ-derivatives and pointwise products, and each

factor differs between the two arguments only by $\Delta U_{\sigma-1}$ or one of its θ-derivatives; the product rule therefore gives

$$\mathcal{M}(U_{\sigma-1})(\theta,\eta) - \mathcal{M}(U_{\sigma-2})(\theta,\eta) = O\left(\eta^{(\sigma-1)\alpha}\right) \qquad \text{as } \eta \to 0^+, \tag{41}$$

with the same bound for every θ-derivative. Applying I_η^α and using (4),

$$\Delta U_\sigma(\theta,\eta) = -I_\eta^\alpha[\mathcal{M}(U_{\sigma-1}) - \mathcal{M}(U_{\sigma-2})](\theta,\eta) = O(\eta^{\sigma\alpha}), \tag{42}$$

completing the induction.

(b) The same induction applies with U in place of $U_{\sigma-1}$. For $N = 0$, $U - U_0 = -I_\eta^\alpha[\mathcal{M}(U)]$, and $\mathcal{M}(U)$ and its θ-derivatives are bounded on $\Omega \times [0, T_1]$, so $U - U_0$ and its θ-derivatives are $O(\eta^\alpha)$. If $U - U_{N-1}$ and its θ-derivatives are $O\left(\eta^{N\alpha}\right)$, the product rule gives the same for $\mathcal{M}(U) - \mathcal{M}(U_{N-1})$, and $U - U_N = -I_\eta^\alpha[\mathcal{M}(U) - \mathcal{M}(U_{N-1})] = O\left(\eta^{(N+1)\alpha}\right)$. □

Remark 7. *Part (a) of Proposition 3 concerns only the iterates and holds unconditionally; it accounts for the power structure $\eta^\alpha, \eta^{2\alpha}, \eta^{3\alpha}, \ldots$ visible in the closed-form iterates of Examples 1 and 2. Part (b) shows that, whenever a smooth solution exists, U_N reproduces it up to and including order $\eta^{N\alpha}$, so that the method behaves like an order-$(N+1)\alpha$ scheme in the time-fractional variable; this is the local counterpart of Theorem 4, and in the classical case $\alpha = 1$ it reduces to the familiar $O\left(\eta^{N+1}\right)$ local truncation error of an N-term Picard iteration. The hypothesis of part (b) is satisfied at $\alpha = 1$ by the exact solutions of Examples 1 and 2, which are smooth traveling waves with all θ-derivatives bounded, so that at $\alpha = 1$ estimate (39) holds for these examples without any appeal to Assumption 2. For $\alpha < 1$ it holds whenever a smooth solution exists, which is precisely the question left open in Remark 6.*

6. Application of the Technique

We now apply the $(\mathrm{AT})^2$ scheme to two initial value problems for the fractional DSW system, chosen so that the classical case $\alpha = 1$ admits a closed-form kink and soliton solution against which the approximations can be measured. The corrections are computed explicitly and compared with those exact profiles in Section 7.

6.1. Example 1

We consider the following fractional Drinfeld–Sokolov–Wilson system

$$\begin{aligned} D_\eta^\alpha \Upsilon(\theta,\eta) &= -3\Phi(\theta,\eta)\Phi_\theta(\theta,\eta), \\ D_\eta^\alpha \Phi(\theta,\eta) &= -2\Phi_{\theta,\theta,\theta}(\theta,\eta) - 2\Upsilon(\theta,\eta)\Phi_\theta(\theta,\eta) - \Upsilon_\theta(\theta,\eta)\Phi(\theta,\eta). \end{aligned} \tag{43}$$

with the initial condition

$$\begin{aligned} \Upsilon(\theta,0) &= \frac{-3}{16}\tanh^2\left(\frac{\theta}{4}\right), \\ \Phi(\theta,0) &= \frac{\sqrt{2}}{8}\tanh\left(\frac{\theta}{4}\right). \end{aligned} \tag{44}$$

Apply the AT to Equation (43) and then the inverse AT to get the following result

$$\begin{aligned} \Upsilon(\theta,\eta) &= \Upsilon(\theta,0) - \varkappa^{-1}\left[\frac{1}{s^\alpha}\{\varkappa[3\Phi(\theta,\eta)\Phi_\theta(\theta,\eta)]\}\right], \\ \Phi(\theta,\eta) &= \Phi(\theta,0) - \varkappa^{-1}\left[\frac{1}{s^\alpha}\{\varkappa[2\Phi_{\theta,\theta,\theta}(\theta,\eta) + 2\Upsilon(\theta,\eta)\Phi_\theta(\theta,\eta) + \Upsilon_\theta(\theta,\eta)\Phi(\theta,\eta)]\}\right]. \end{aligned} \tag{45}$$

When we use the TAM approach, we get

$$\begin{aligned} \Upsilon_0(\theta,0) &= \frac{-3}{16}\tanh^2\left(\frac{\theta}{4}\right), \\ \Phi_0(\theta,0) &= \frac{\sqrt{2}}{8}\tanh\left(\frac{\theta}{4}\right). \end{aligned} \tag{46}$$

Likewise, the remaining iteration may be computed for $\sigma \geq 1$ in the same way. The approximate solution to the problem is represented by each iteration

$$\begin{aligned} \Upsilon_\sigma(\theta,\eta) &= \Upsilon_0(\theta,0) - \varkappa^{-1}\left[\frac{1}{s^\alpha}\{\varkappa[3\Phi_{\sigma-1}(\theta,\eta)(\Phi_{\sigma-1})_\theta(\theta,\eta)]\}\right], \\ \Phi_\sigma(\theta,\eta) &= \Phi_0(\theta,0) - \varkappa^{-1}\left[\frac{1}{s^\alpha}\left\{\varkappa\left[2(\Phi_{\sigma-1})_{\theta,\theta,\theta}(\theta,\eta) + 2(\Upsilon_{\sigma-1})(\theta,\eta)(\Phi_{\sigma-1})_\theta(\theta,\eta) + (\Upsilon_{\sigma-1})_\theta(\theta,\eta)\Phi_{\sigma-1}(\theta,\eta)\right]\right\}\right]. \end{aligned} \tag{47}$$

The exact solution of Section 6.1 (Example 1) is reached by $\Upsilon_\sigma(\theta,\eta)$ and $\Phi_\sigma(\theta,\eta)$ when $\sigma \to \infty$ as

$$\Upsilon_1(\theta,\eta) = \Upsilon_0(\theta,0) - \frac{3\eta^\alpha \tanh\left(\frac{\theta}{4}\right)\operatorname{sech}^2\left(\frac{\theta}{4}\right)}{128\Gamma(\alpha+1)}, \tag{48}$$

$$\Upsilon_2(\theta,\eta) = \Upsilon_1(\theta,\eta) + \frac{3\eta^{2\alpha}\left(\cosh\left(\frac{\theta}{2}\right)-2\right)\operatorname{sech}^4\left(\frac{\theta}{4}\right)}{2048\Gamma(2\alpha+1)} + \frac{3\Gamma(2\alpha+1)\eta^{3\alpha}\tanh\left(\frac{\theta}{4}\right)\operatorname{sech}^4\left(\frac{\theta}{4}\right)}{16384\Gamma(\alpha+1)^2\Gamma(3\alpha+1)}, \cdots, \tag{49}$$

$$\Phi_1(\theta,\eta) = \Phi_0(\theta,0) + \frac{\eta^\alpha \operatorname{sech}^2\left(\frac{\theta}{4}\right)}{64\sqrt{2}\Gamma(\alpha+1)}, \tag{50}$$

$$\Phi_2(\theta,\eta) = \Phi_1(\theta,\eta) - \frac{\eta^{2\alpha}\tanh\left(\frac{\theta}{4}\right)\operatorname{sech}^2\left(\frac{\theta}{4}\right)}{512\sqrt{2}\Gamma(2\alpha+1)} - \frac{3\Gamma(2\alpha+1)\eta^{3\alpha}\left(3\cosh\left(\frac{\theta}{2}\right)-4\right)\operatorname{sech}^6\left(\frac{\theta}{4}\right)}{32768\sqrt{2}\Gamma(\alpha+1)^2\Gamma(3\alpha+1)}, \cdots,$$

For $\alpha = 1$, the exact solution to the aforementioned is

$$\begin{aligned} \Upsilon(\theta,\eta) &= \frac{-3}{16}\tanh^2\left(\frac{1}{4}\left(\theta+\frac{\eta}{4}\right)\right), \\ \Phi(\theta,\eta) &= \frac{\sqrt{2}}{8}\tanh\left(\frac{1}{4}\left(\theta+\frac{\eta}{4}\right)\right). \end{aligned} \tag{51}$$

6.2. Example 2

We consider the following the following fractional Drinfeld–Sokolov–Wilson system

$$\begin{aligned} D_\eta^\alpha \Upsilon(\theta,\eta) &= -3\Phi(\theta,\eta)\Phi_\theta(\theta,\eta), \\ D_\eta^\alpha \Phi(\theta,\eta) &= -2\Phi_{\theta,\theta,\theta}(\theta,\eta) - 2\Upsilon(\theta,\eta)\Phi_\theta(\theta,\eta) - \Upsilon_\theta(\theta,\eta)\Phi(\theta,\eta). \end{aligned} \tag{52}$$

with the initial condition

$$\begin{aligned} \Upsilon(\theta,0) &= \frac{3c}{2}\operatorname{sech}^2\left(\sqrt{\frac{c}{2}}\theta\right), \\ \Phi(\theta,0) &= c\,\operatorname{sech}\left(\sqrt{\frac{c}{2}}\theta\right). \end{aligned} \tag{53}$$

Apply the AT to Equation (52) and then the inverse AT to get the following result

$$\begin{aligned}\Upsilon(\theta,\eta) &= \Upsilon(\theta,0)-\varkappa^{-1}\left[\frac{1}{s^{\alpha}}\{\varkappa[3\Phi(\theta,\eta)\Phi_{\theta}(\theta,\eta)]\}\right],\\ \Phi(\theta,\eta) &= \Phi(\theta,0)-\varkappa^{-1}\left[\frac{1}{s^{\alpha}}\{\varkappa[2\Phi_{\theta,\theta,\theta}(\theta,\eta)+2\Upsilon(\theta,\eta)\Phi_{\theta}(\theta,\eta)+\Upsilon_{\theta}(\theta,\eta)\Phi(\theta,\eta)]\}\right].\end{aligned} \tag{54}$$

When we use the TAM approach, we get

$$\begin{aligned}\Upsilon_0(\theta,0) &= \frac{3c}{2}\operatorname{sech}^2\left(\sqrt{\frac{c}{2}}\theta\right),\\ \Phi_0(\theta,0) &= c\operatorname{sech}\left(\sqrt{\frac{c}{2}}\theta\right).\end{aligned} \tag{55}$$

Likewise, the remaining iteration may be computed for $\sigma \geq 1$ in the same way. The approximate solution to the problem is represented by each iteration

$$\begin{aligned}\Upsilon_{\sigma}(\theta,\eta) &= \Upsilon_0(\theta,0)-\varkappa^{-1}\left[\frac{1}{s^{\alpha}}\{\varkappa[3\Phi_{\sigma-1}(\theta,\eta)(\Phi_{\sigma-1})_{\theta}(\theta,\eta)]\}\right],\\ \Phi_{\sigma}(\theta,\eta) &= \Phi_0(\theta,0)-\varkappa^{-1}\left[\frac{1}{s^{\alpha}}\left\{\varkappa\left[2(\Phi_{\sigma-1})_{\theta,\theta,\theta}(\theta,\eta)+2(\Upsilon_{\sigma-1})(\theta,\eta)(\Phi_{\sigma-1})_{\theta}(\theta,\eta)+(\Upsilon_{\sigma-1})_{\theta}(\theta,\eta)\Phi_{\sigma-1}(\theta,\eta)\right]\right\}\right].\end{aligned} \tag{56}$$

The exact solution of Section 6.2 (Example 2) is reached by $\Upsilon_{\sigma}(\theta,\eta)$ and $\Phi_{\sigma}(\theta,\eta)$ when $\sigma \to \infty$ as

$$\Upsilon_1(\theta,\eta) = \Upsilon_0(\theta,0)+\frac{3c^{5/2}\eta^{\alpha}\tanh\left(\frac{\sqrt{c}\theta}{\sqrt{2}}\right)\operatorname{sech}^2\left(\frac{\sqrt{c}\theta}{\sqrt{2}}\right)}{\sqrt{2}\Gamma(\alpha+1)}, \tag{57}$$

$$\begin{aligned}\Upsilon_2(\theta,\eta) &= \Upsilon_1(\theta,\eta)+\frac{3c^4\eta^{2\alpha}\left(\cosh\left(\sqrt{2}\sqrt{c}\theta\right)-2\right)\operatorname{sech}^4\left(\frac{\sqrt{c}\theta}{\sqrt{2}}\right)}{2\Gamma(2\alpha+1)}\\ &\quad+\frac{3c^{11/2}\Gamma(2\alpha+1)\eta^{3\alpha}\left(\sinh\left(\frac{3\sqrt{c}\theta}{\sqrt{2}}\right)-7\sinh\left(\frac{\sqrt{c}\theta}{\sqrt{2}}\right)\right)\operatorname{sech}^5\left(\frac{\sqrt{c}\theta}{\sqrt{2}}\right)}{8\sqrt{2}\Gamma(\alpha+1)^2\Gamma(3\alpha+1)},\cdots,\end{aligned} \tag{58}$$

$$\Phi_1(\theta,\eta) = \Phi_0(\theta,0)+\frac{c^{5/2}\eta^{\alpha}\tanh\left(\frac{\sqrt{c}\theta}{\sqrt{2}}\right)\operatorname{sech}\left(\frac{\sqrt{c}\theta}{\sqrt{2}}\right)}{\sqrt{2}\Gamma(\alpha+1)}, \tag{59}$$

$$\begin{aligned}\Phi_2(\theta,\eta) &= \Phi_1(\theta,\eta)+\frac{c^4\eta^{2\alpha}\left(\cosh\left(\sqrt{2}\sqrt{c}\theta\right)-3\right)\operatorname{sech}^3\left(\frac{\sqrt{c}\theta}{\sqrt{2}}\right)}{4\Gamma(2\alpha+1)}\\ &\quad+\frac{3c^{11/2}\Gamma(2\alpha+1)\eta^{3\alpha}\left(\sinh\left(\frac{3\sqrt{c}\theta}{\sqrt{2}}\right)-6\sinh\left(\frac{\sqrt{c}\theta}{\sqrt{2}}\right)\right)\operatorname{sech}^6\left(\frac{\sqrt{c}\theta}{\sqrt{2}}\right)}{2\sqrt{2}\Gamma(\alpha+1)^2\Gamma(3\alpha+1)},\cdots,\end{aligned} \tag{60}$$

For $\alpha = 1$, the exact solution to the aforementioned is

$$\begin{aligned}\Upsilon(\theta,\eta) &= \frac{3c}{2}\operatorname{sech}^2\left(\sqrt{\frac{c}{2}}(\theta-c\eta)\right),\\ \Phi(\theta,\eta) &= c\ \operatorname{sech}\left(\sqrt{\frac{c}{2}}(\theta-c\eta)\right).\end{aligned} \tag{61}$$

7. Numerical Results and Discussion

Both examples were chosen so that the classical case $\alpha = 1$ has a closed-form solution, which allows the $(\mathrm{AT})^2$ approximations to be measured against an exact profile rather than judged by appearance. Throughout, the approximation is the second iterate $U_2 = (\mathrm{Y}_2, \Phi_2)$ derived in Section 6. As a reference we use the Adomian decomposition method (ADM) [20] with the same number of corrections, which by Remark 3 coincides with its Laplace-transform variant, that is, its third partial sum, computed for the same data. Tables 2–5 report absolute and relative errors at $\eta = 0.1$, and Figures 1–6 show the approximate solutions, their errors over longer times, and the effect of the fractional order.

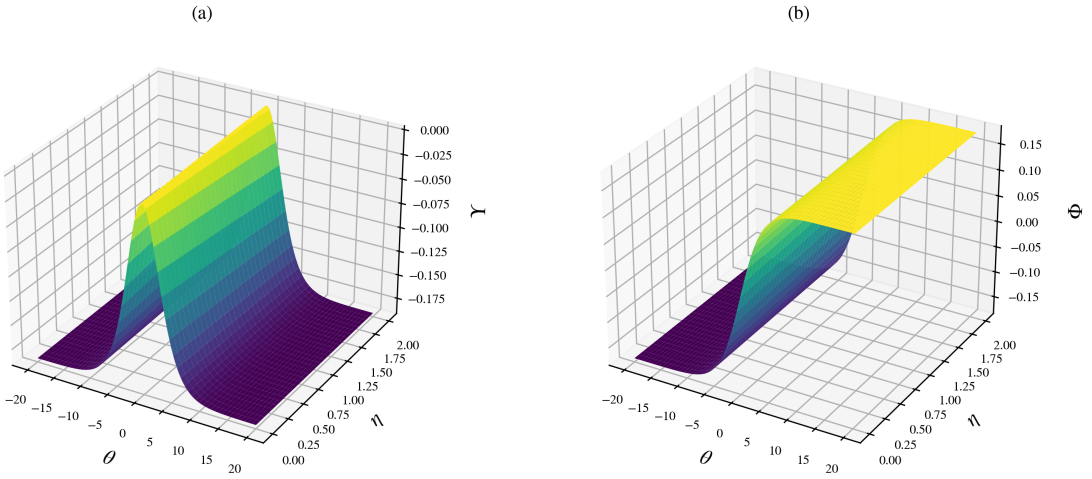


Figure 1. 3D surfaces of the approximations Y_2 and Φ_2 for Section 6.1 (Example 1).

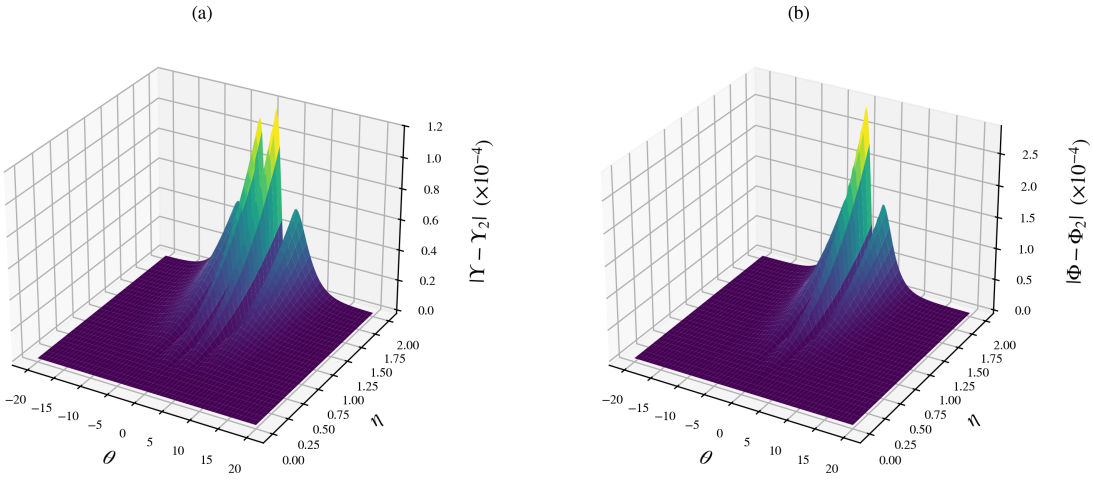


Figure 2. Absolute errors of $|\mathrm{Y} - \mathrm{Y}_2|$ and $|\Phi - \Phi_2|$ at $\alpha = 1$ for Section 6.1 (Example 1).

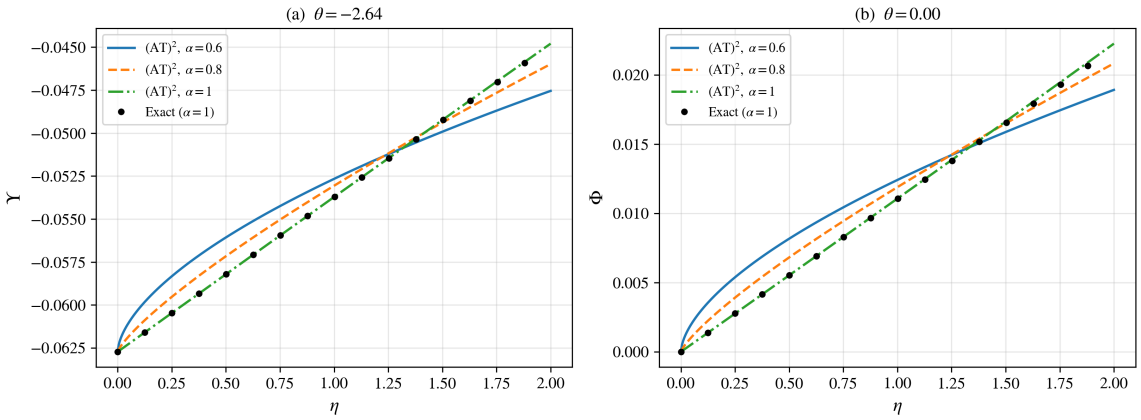


Figure 3. Effect of the fractional order on the time evolution of Υ at $\theta = -2.64$ and Φ at $\theta = 0$ for Section 6.1 (Example 1).

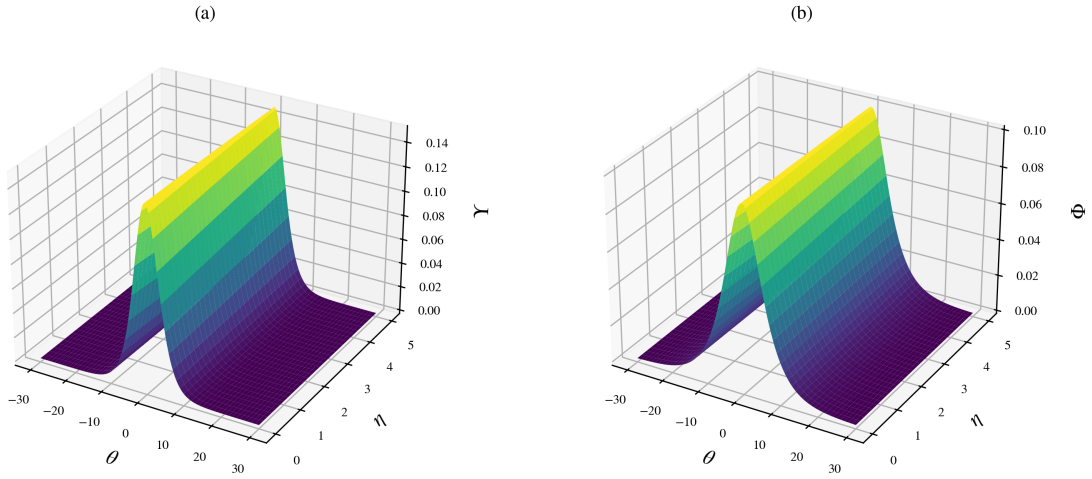


Figure 4. 3D surfaces of the approximations Υ_2 and Φ_2 for Section 6.2 (Example 2).

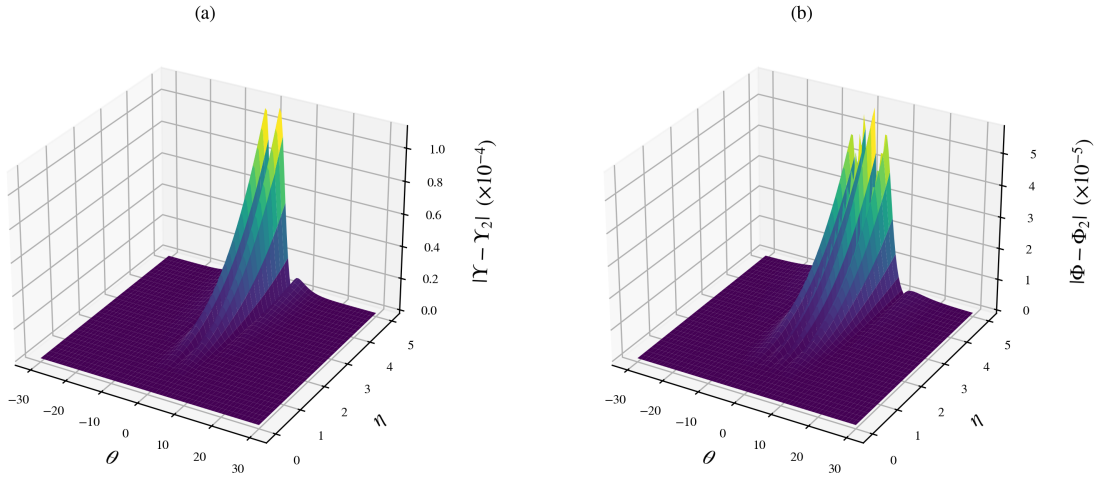


Figure 5. Absolute errors of $|\Upsilon - \Upsilon_2|$ and $|\Phi - \Phi_2|$ at $\alpha = 1$ for Section 6.2 (Example 2).

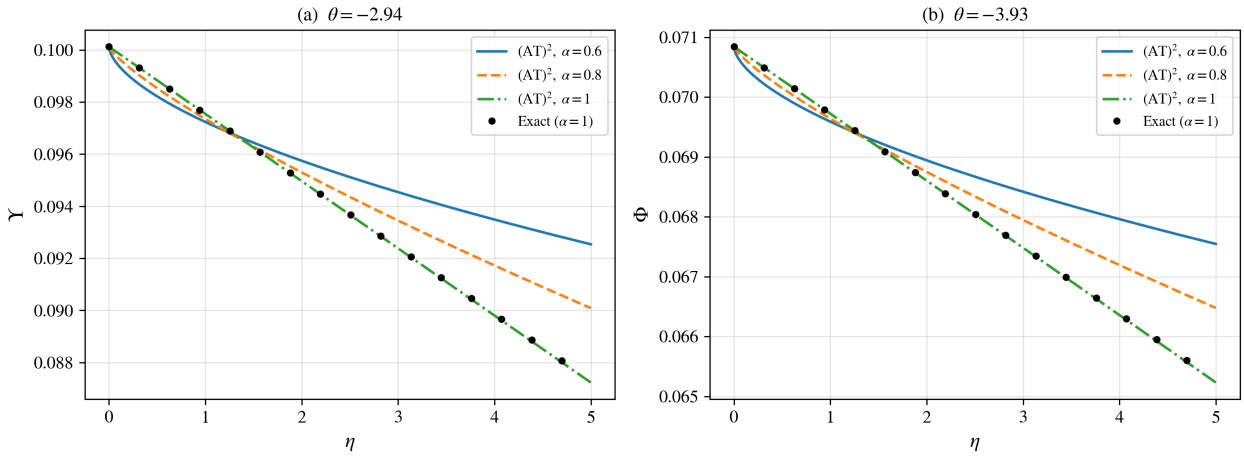


Figure 6. Effect of the fractional order on the time evolution of Υ at $\theta = -2.94$ and Φ at $\theta = -3.93$ for Section 6.2 (Example 2).

Table 2. Comparison between the exact solution, $(AT)^2$ and ADM for Section 6.1 (Example 1) $(\Upsilon(\theta, \eta))$ at $\eta = 0.1$.

			$(AT)^2$		ADM	
θ	**Exact**	$(AT)^2$	**Abs. Error**	**Rel. Error**	**Abs. Error**	**Rel. Error**
3	−0.076527	−0.076527	4.38×10^{-9}	5.72×10^{-8}	1.82×10^{-8}	2.37×10^{-7}
6	−0.153999	−0.153999	6.38×10^{-9}	4.14×10^{-8}	4.57×10^{-9}	2.97×10^{-8}
9	−0.179449	−0.179449	2.36×10^{-9}	1.32×10^{-8}	2.25×10^{-9}	1.25×10^{-8}
12	−0.185673	−0.185673	5.86×10^{-10}	3.15×10^{-9}	5.80×10^{-10}	3.12×10^{-9}
15	−0.187091	−0.187091	1.34×10^{-10}	7.15×10^{-10}	1.33×10^{-10}	7.13×10^{-10}
18	−0.187409	−0.187409	3.00×10^{-11}	1.60×10^{-10}	3.00×10^{-11}	1.60×10^{-10}
21	−0.187480	−0.187480	6.70×10^{-12}	3.57×10^{-11}	6.70×10^{-12}	3.57×10^{-11}
24	−0.187495	−0.187495	1.50×10^{-12}	7.97×10^{-12}	1.50×10^{-12}	7.97×10^{-12}
27	−0.187499	−0.187499	3.34×10^{-13}	1.78×10^{-12}	3.34×10^{-13}	1.78×10^{-12}
30	−0.187500	−0.187500	7.45×10^{-14}	3.97×10^{-13}	7.45×10^{-14}	3.97×10^{-13}

The parameter values were chosen as follows. The tables use $\alpha = 1$, the only order for which an exact solution is available, so that the error can be measured rather than estimated. They use $\eta = 0.1$, a time close to the initial instant, which is where the local truncation estimate of Proposition 3 applies and where the existence result of Theorem 2 is local (Remark 5); this is also comparable to the time ranges used for these examples in [32,43]. For the soliton we take $c = 0.1$, for which the corrections, homogeneous in c, are small; by the scaling symmetry discussed below, the results for other values of c follow. In the figures the time interval is longer, $\eta \leq 2$ for Section 6.1 (Example 1) and $\eta \leq 5$ for Section 6.2 (Example 2), so that the motion of the wave is visible while the error of the two-correction truncation stays below 3×10^{-4}; for Section 6.2 (Example 2) the longer interval compensates for the slow speed $c = 0.1$. The fractional orders $\alpha = 0.6$, 0.8 and 1 span the interval $0 < \alpha \leq 1$ widely enough for the memory effect to be clearly visible.

Table 3. Comparison between the exact solution, $(\mathrm{AT})^2$ and ADM for Section 6.1 (Example 1) $(\Phi(\theta,\eta))$ at $\eta = 0.1$.

		$(\mathrm{AT})^2$			ADM	
θ	Exact	$(\mathrm{AT})^2$	Abs. Error	Rel. Error	Abs. Error	Rel. Error
3	0.112936	0.112936	1.58×10^{-8}	1.40×10^{-7}	1.83×10^{-9}	1.62×10^{-8}
6	0.160208	0.160208	7.12×10^{-9}	4.44×10^{-8}	3.78×10^{-9}	2.36×10^{-8}
9	0.172940	0.172940	1.40×10^{-9}	8.08×10^{-9}	1.17×10^{-9}	6.74×10^{-9}
12	0.175913	0.175913	2.91×10^{-10}	1.66×10^{-9}	2.79×10^{-10}	1.58×10^{-9}
15	0.176584	0.176584	6.38×10^{-11}	3.61×10^{-10}	6.32×10^{-11}	3.58×10^{-10}
18	0.176734	0.176734	1.42×10^{-11}	8.02×10^{-11}	1.41×10^{-11}	8.00×10^{-11}
21	0.176767	0.176767	3.16×10^{-12}	1.79×10^{-11}	3.16×10^{-12}	1.79×10^{-11}
24	0.176775	0.176775	7.05×10^{-13}	3.99×10^{-12}	7.05×10^{-13}	3.99×10^{-12}
27	0.176776	0.176776	1.57×10^{-13}	8.90×10^{-13}	1.57×10^{-13}	8.90×10^{-13}
30	0.176777	0.176777	3.51×10^{-14}	1.99×10^{-13}	3.51×10^{-14}	1.99×10^{-13}

Table 4. Comparison between the exact solution, $(\mathrm{AT})^2$ and ADM for Section 6.2 (Example 2) $(\mathrm{Y}(\theta,\eta))$ at $\eta = c = 0.1$.

		$(\mathrm{AT})^2$			ADM	
θ	Exact	$(\mathrm{AT})^2$	Abs. Error	Rel. Error	Abs. Error	Rel. Error
3	0.098833	0.098833	7.02×10^{-10}	7.10×10^{-9}	8.37×10^{-10}	8.47×10^{-9}
6	0.036066	0.036066	9.59×10^{-12}	2.66×10^{-10}	1.31×10^{-10}	3.64×10^{-9}
9	0.010391	0.010391	5.40×10^{-11}	5.19×10^{-9}	1.18×10^{-10}	1.14×10^{-8}
12	0.002788	0.002788	1.90×10^{-11}	6.82×10^{-9}	3.88×10^{-11}	1.39×10^{-8}
15	7.3399×10^{-4}	7.3399×10^{-4}	5.34×10^{-12}	7.27×10^{-9}	1.07×10^{-11}	1.46×10^{-8}
18	1.9223×10^{-4}	1.9223×10^{-4}	1.42×10^{-12}	7.39×10^{-9}	2.84×10^{-12}	1.48×10^{-8}
21	5.0275×10^{-5}	5.0275×10^{-5}	3.73×10^{-13}	7.43×10^{-9}	7.46×10^{-13}	1.48×10^{-8}
24	1.3144×10^{-5}	1.3144×10^{-5}	9.77×10^{-14}	7.43×10^{-9}	1.95×10^{-13}	1.49×10^{-8}
27	3.4362×10^{-6}	3.4362×10^{-6}	2.56×10^{-14}	7.44×10^{-9}	5.10×10^{-14}	1.49×10^{-8}
30	8.9830×10^{-7}	8.9830×10^{-7}	6.68×10^{-15}	7.44×10^{-9}	1.33×10^{-14}	1.49×10^{-8}

Two remarks on the data are needed, because both examples appear in the literature in forms that are not consistent with the system. In Section 6.1 (Example 1) the initial condition for Φ is $\frac{\sqrt{2}}{8}\tanh(\theta/4)$. It is printed as $\tanh^2(\theta/4)$ in [56], but the exact solution and the errors reported there correspond to $\tanh(\theta/4)$, and with $\tanh^2$ the stated profile does not satisfy (43). In Section 6.2 (Example 2) the amplitude of Y must be $+\frac{3c}{2}$; with the negative sign that also appears in the literature [32], the sech^2 profile is not a solution. As an independent check on both the data and the implementation, we note that at $\alpha = 1$ the $(\mathrm{AT})^2$ recursion coincides with the variational iteration method with Lagrange multiplier -1, and its third iterate reproduces the absolute errors reported for Section 6.1 (Example 1) in [56] at the points used there.

Table 5. Comparison between the exact solution, $(AT)^2$ and ADM for Section 6.2 (Example 2) ($\Phi(\theta, \eta)$) at $\eta = c = 0.1$.

			$(AT)^2$		ADM	
θ	Exact	$(AT)^2$	Abs. Error	Rel. Error	Abs. Error	Rel. Error
3	0.081172	0.081172	5.11×10^{-11}	6.30×10^{-10}	2.60×10^{-10}	3.21×10^{-9}
6	0.049034	0.049034	3.00×10^{-10}	6.13×10^{-9}	3.49×10^{-11}	7.11×10^{-10}
9	0.026319	0.026319	4.11×10^{-11}	1.56×10^{-9}	2.77×10^{-11}	1.05×10^{-9}
12	0.013634	0.013634	1.15×10^{-11}	8.46×10^{-10}	2.23×10^{-11}	1.64×10^{-9}
15	0.006995	0.006995	1.11×10^{-11}	1.59×10^{-9}	1.26×10^{-11}	1.80×10^{-9}
18	0.003580	0.003580	6.40×10^{-12}	1.79×10^{-9}	6.60×10^{-12}	1.84×10^{-9}
21	0.001831	0.001831	3.37×10^{-12}	1.84×10^{-9}	3.40×10^{-12}	1.86×10^{-9}
24	9.3610×10^{-4}	9.3610×10^{-4}	1.74×10^{-12}	1.86×10^{-9}	1.74×10^{-12}	1.86×10^{-9}
27	4.7863×10^{-4}	4.7863×10^{-4}	8.90×10^{-13}	1.86×10^{-9}	8.90×10^{-13}	1.86×10^{-9}
30	2.4472×10^{-4}	2.4472×10^{-4}	4.55×10^{-13}	1.86×10^{-9}	4.55×10^{-13}	1.86×10^{-9}

For Section 6.1 (Example 1), Tables 2 and 3 show that two corrections already give absolute errors of at most 6.4×10^{-9} in Y and 1.6×10^{-8} in Φ, attained near the core of the kink, falling to 7.4×10^{-14} and 3.5×10^{-14} at $\theta = 30$. The relative errors never exceed 5.7×10^{-8} and 1.4×10^{-7}, respectively, so the small absolute errors do not reflect small values of the solution. The error follows the hyperbolic factors in the corrections: it is largest where the profile changes fastest and decays as these factors approach their asymptotic values. The decay is not strictly monotone; the error in Y is larger at $\theta = 6$ than at $\theta = 3$, because the leading neglected term is a combination of hyperbolic functions whose dependence on θ has interior maxima and zeros.

The comparison with ADM is easiest to read through the structure of the two approximations. At $\alpha = 1$ both reproduce the Taylor expansion of the exact solution in η up to and including η^2. The ADM sum stops there, whereas U_2 also contains part of the η^3 term, generated by the products in $\mathcal{M}(U_1)$. Away from the kink the η^3 coefficient is negligible, and the two methods agree to within a few per cent for $\theta \geq 12$ and to the digits shown for $\theta \geq 21$. Near the core the partial term may help or not: at $\theta = 3$ the $(AT)^2$ error in Y is four times smaller than that of ADM, while the ADM error in Φ is about nine times smaller. Neither method is uniformly more accurate.

Figures 1–3 extend the picture beyond the single instant of the tables. In Figure 1 the well in Y and the kink in Φ translate in the negative θ direction with speed $\frac{1}{4}$ over $0 \leq \eta \leq 2$, and at this scale the approximations cannot be distinguished from (51). The error surfaces in Figure 2 grow with η and reach 1.2×10^{-4} in Y and 2.9×10^{-4} in Φ at $\eta = 2$, concentrated around the core. This growth is what part (b) of Proposition 3 predicts, since at $\alpha = 1$ the truncation error after two corrections is $O(\eta^3)$, and it is consistent with Remark 5: a two-correction truncation is accurate near the initial time and loses accuracy as η increases. Figure 3 follows Y at $\theta = -2.64$ and Φ at $\theta = 0$, the points where the nonlinear term is largest at $\eta = 0$. The curve for $\alpha = 1$ coincides with the exact solution. For $\alpha < 1$ the solution moves away from its initial value faster at small η and more slowly afterwards, crossing the classical curve near $\eta \approx 1.3$. This is the effect of the weight $\eta^\alpha / \Gamma(\alpha + 1)$ in the first correction, which is steeper than linear near $\eta = 0$ and flatter later, and it is the signature of the memory carried by the Caputo derivative.

For Section 6.2 (Example 2) with $c = 0.1$, Tables 4 and 5 show smaller errors still: at most 7.0×10^{-10} in Y and 3.0×10^{-10} in Φ, decreasing to 6.7×10^{-15} and 4.6×10^{-13} at $\theta = 30$, with relative errors below 7.4×10^{-9} and 6.1×10^{-9}. Here the $(AT)^2$ error in Y is

smaller than that of ADM at every point, typically by a factor of two and by more than an order of magnitude at $\theta = 6$, while for Φ the comparison is again mixed and the two methods agree closely for $\theta \geq 18$. The size of the errors is governed by c. The corrections are homogeneous in the wave-speed parameter, with $\mathrm{Y}_1 - \mathrm{Y}_0$ proportional to $c^{5/2}$ and the terms of $\mathrm{Y}_2 - \mathrm{Y}_1$ proportional to c^4 and $c^{11/2}$, and similarly for Φ. These are the powers forced by the scaling symmetry noted in Section 2, so the results reported for $c = 0.1$ determine those for every $c > 0$; a larger c corresponds to a faster and narrower soliton and to larger errors at a fixed point (θ, η).

In Figure 4 the soliton moves to the right with speed c, so it travels only half a unit over $0 \leq \eta \leq 5$ and appears nearly stationary at this scale, as expected for $c = 0.1$. The error surfaces in Figure 5 reach 1.1×10^{-4} in Y and 5.7×10^{-5} in Φ at $\eta = 5$ and are concentrated around the pulse, where it changes fastest as it moves. Figure 6 follows the two components at $\theta = -2.94$ and $\theta = -3.93$, on the rear flank of the pulse, where the values decrease as the pulse moves away. The fractional order acts as in Section 6.1 (Example 1): for $\alpha < 1$ the decrease is faster at first and slower later, with the curves crossing the classical one slightly above $\eta = 1$.

Taken together, the two examples show that two corrections suffice for errors of order 10^{-8} or smaller at $\eta = 0.1$, distributed according to the local size of the nonlinear terms rather than uniformly in θ. The accuracy is comparable to that of ADM with the same number of corrections, and the ADM partial sum is also somewhat cheaper to form, since it omits the partial $\eta^{3\alpha}$ term. The advantage of the $(\mathrm{AT})^2$ scheme is therefore not computational but structural: it is a Picard iteration for the Volterra formulation, and this is what gives access to the convergence theory of Section 5. Two limitations should be kept in mind. The experiments do not verify Theorems 3 and 4 for the DSW system, which apply only under Assumption 2, a condition that, by Remark 6, fails in the classical function spaces. And for $\alpha < 1$, where no exact solution is available, the curves in Figures 3 and 6 are approximations whose accuracy is not measured directly.

8. Conclusions

In this work we studied the time-fractional Drinfeld–Sokolov–Wilson system in the Caputo sense and solved it by combining the Aboodh transform with the Temimi–Ansari iteration, a hybrid we refer to as the $(\mathrm{AT})^2$ method. The scheme resolves the nonlinear coupling without auxiliary polynomials or an embedding parameter, by evaluating the nonlinear operator directly on the preceding iterate. We showed that its iterates are exactly the Picard iterates of an equivalent fractional Volterra integral equation, and that they do not depend on the choice of a Laplace-type transform. Under a Lipschitz condition on the nonlinear operator this gives existence and uniqueness of a local solution by the Banach fixed-point theorem, together with an explicit truncation bound that decays both in the number of iterations and as a power of time, while a local truncation estimate holds for the iterates themselves without any such condition. We also showed that the DSW operator does not satisfy the Lipschitz condition in the classical spaces of bounded smooth functions, because its dispersive term loses three derivatives. The well-posedness of the fractional DSW system therefore remains open, and the analysis identifies what a proof would require: a setting in which the dispersive term is controlled, for instance through its Mittag–Leffler solution operator.

For two benchmark problems of kink and soliton type, whose data we corrected after finding them inconsistent with the system in the literature, two iterations reproduce the classical exact solutions with errors of order 10^{-8} or smaller near the initial time, concentrated where the nonlinear coupling is strongest. The accuracy is comparable to that of the Adomian decomposition method with the same number of corrections. The value of

the $(AT)^2$ scheme therefore lies less in computational economy than in its structure, which connects a practical iteration to the existence theory of fractional Volterra equations and makes clear what remains to be proved for dispersive systems of this kind.

Author Contributions: Conceptualization, A.H.; methodology, A.H. and A.A.; software, A.H.; validation, A.H. and A.A.; formal analysis, A.H.; investigation, A.H. and A.A.; resources, A.A.; data curation, A.H. and A.A.; writing—original draft preparation, A.H. and A.A.; writing—review and editing, A.H.; visualization, A.H. and A.A.; supervision, A.H.; project administration, A.H.; funding acquisition, A.A. All authors have read and agreed to the published version of the manuscript.

Funding: Princess Nourah bint Abdulrahman University Researchers Supporting Project number (PNURSP2026R742), Princess Nourah bint Abdulrahman University, Riyadh, Saudi Arabia.

Data Availability Statement: No new data were created or analyzed in this study. Data sharing is not applicable to this study.

Conflicts of Interest: The authors declare no conflict of interest.

References

1. Podlubny, I. *Fractional Differential Equations: An Introduction to Fractional Derivatives, Fractional Differential Equations, to Methods of Their Solution and Some of Their Applications*; Elsevier: Amsterdam, The Netherlands, 1998; Volume 198.
2. Drinfel'd, V.G.; Sokolov, V.V. Equations of Korteweg–de Vries Type and Simple Lie Algebras. *Dokl. Akad. Nauk. SSSR* **1981**, *258*, 11–16.
3. Wilson, G. The Modified Lax and Two-Dimensional Toda Lattice Equations Associated with Simple Lie Algebras. *Ergod. Theory Dyn. Syst.* **1981**, *1*, 361–380. [CrossRef]
4. Hirota, R.; Grammaticos, B.; Ramani, A. Soliton Structure of the Drinfel'd–Sokolov–Wilson Equation. *J. Math. Phys.* **1986**, *27*, 1499–1505. [CrossRef]
5. Naz, R. Conservation Laws for a Complexly Coupled KdV System, Coupled Burgers' System and Drinfeld–Sokolov–Wilson System via Multiplier Approach. *Commun. Nonlinear Sci. Numer. Simul.* **2010**, *15*, 1177–1182. [CrossRef]
6. Wang, G.w.; Xu, T.z.; Feng, T. Lie Symmetry Analysis and Explicit Solutions of the Time Fractional Fifth-Order KdV Equation. *PLoS ONE* **2014**, *9*, e88336. [CrossRef] [PubMed]
7. Akbulut, A.; Taşcan, F. Lie Symmetries, Symmetry Reductions and Conservation Laws of Time Fractional Modified Korteweg–de Vries (mKdV) Equation. *Chaos Solitons Fractals* **2017**, *100*, 1–6. [CrossRef]
8. Sil, S.; Raja Sekhar, T.; Zeidan, D. Lie Symmetry Analysis and Exact Solutions of the Time-Fractional Biological Population Model. *Phys. A Stat. Mech. Its Appl.* **2020**, *540*, 123134. [CrossRef]
9. Zinat, N.; Hussain, A.; Kara, A.H.; Zaman, F.D. On the Analysis and Integrability of the Time-Fractional Stochastic Potential-KdV Equation. *Quaest. Math.* **2025**, *48*, 909–928. [CrossRef]
10. Ali, M.; Gandhi, H.; Tomar, A.; Singh, D. Similarity Solution for a System of Fractional-Order Coupled Nonlinear Hirota Equations with Conservation Laws. *Mathematics* **2023**, *11*, 2465. [CrossRef]
11. Sahoo, S.; Saha Ray, S. Invariant Analysis with Conservation Laws for the Time Fractional Drinfeld–Sokolov–Satsuma–Hirota Equations. *Chaos Solitons Fractals* **2017**, *104*, 725–733. [CrossRef]
12. Beenish; Alsharidi, A.K. Lie Symmetry, Conservation Laws, and Dynamical Analysis of Ionic Currents in the Microtubule Model. *Mathematics* **2025**, *13*, 3891. [CrossRef]
13. San, S.; Alshammari, F.S. Analytical and Dynamical Study of Solitary Waves in a Fractional Magneto-Electro-Elastic System. *Fractal Fract.* **2025**, *9*, 309. [CrossRef]
14. Khan, A.; Alshammari, F.S.; Yasin, S. Exact Solitary Wave Solutions and Sensitivity Analysis of the Fractional (3+1)D KdV–ZK Equation. *Fractal Fract.* **2025**, *9*, 476. [CrossRef]
15. Biazar, J.; Ayati, Z. Exp and Modified Exp Function Methods for Nonlinear Drinfeld–Sokolov System. *J. King Saud Univ.–Sci.* **2012**, *24*, 315–318. [CrossRef]
16. Arnous, A.H.; Mirzazadeh, M.; Eslami, M. Exact Solutions of the Drinfel'd–Sokolov–Wilson Equation Using Bäcklund Transformation of Riccati Equation and Trial Function Approach. *Pramana* **2016**, *86*, 1153–1160. [CrossRef]
17. Hossain, M.N.; Miah, M.M.; Alosaimi, M.; Alsharif, F.; Kanan, M. Exploring Novel Soliton Solutions to the Time-Fractional Coupled Drinfel'd–Sokolov–Wilson Equation in Industrial Engineering Using Two Efficient Techniques. *Fractal Fract.* **2024**, *8*, 352. [CrossRef]
18. Shahen, N.H.M.; Al Amin, M.; Foyjonnesa; Rahman, M.M. Soliton Structures of Fractional Coupled Drinfel'd–Sokolov–Wilson Equation Arising in Water Wave Mechanics. *Sci. Rep.* **2024**, *14*, 18894. [CrossRef] [PubMed]

19. Patel, Y.F.; Izadi, M. Analytical study of the fractional-order Drinfeld–Sokolov–Wilson system for nonlinear wave dynamics in dispersive media with modulation instability analysis. *Arab. J. Math.* **2026**, *15*, 331–348. [CrossRef]
20. Adomian, G. *Solving Frontier Problems of Physics: The Decomposition Method*; Kluwer Academic Publishers: Dordrecht, The Netherlands, 1994.
21. He, J.H. Variational Iteration Method—A Kind of Non-Linear Analytical Technique: Some Examples. *Int. J.-Non-Linear Mech.* **1999**, *34*, 699–708. [CrossRef]
22. Ali, N.; Zada, L.; Nawaz, R.; Jamshed, W.; Ibrahim, R.W.; Guedri, K.; Khalifa, H.A.E.W. Analysis and Simulation of Arbitrary Order Shallow Water and Drinfeld–Sokolov–Wilson Equations: Natural Transform Decomposition Method. *Int. J. Mod. Phys. B* **2024**, *38*, 2450088. [CrossRef]
23. Al-Rozbayani, A.M.; Ali, A.H. Applied Sumudu Transform with Adomian Decomposition Method to the Coupled Drinfeld–Sokolov–Wilson System. *Al-Rafidain J. Comput. Sci. Math.* **2021**, *15*, 139–147. [CrossRef]
24. Algahtani, O.; Saifullah, S.; Ali, A. Semi-Analytical and Numerical Study of Fractal Fractional Nonlinear System Under Caputo Fractional Derivative. *AIMS Math.* **2022**, *7*, 16760–16774. [CrossRef]
25. Singh, P.K.; Vishal, K.; Som, T. Solution of Fractional Drinfeld–Sokolov–Wilson Equation Using Homotopy Perturbation Transform Method. *Appl. Appl. Math. Int. J.* **2015**, *10*, 460–472.
26. Nadeem, M.; Alsayaad, Y.; Adel, W. A New Study for the Investigation of Nonlinear Fractional Drinfeld–Sokolov–Wilson Equation. *Math. Probl. Eng.* **2023**, *2023*, 9274115. [CrossRef]
27. Singh, J.; Kumar, D.; Baleanu, D.; Rathore, S. An Efficient Numerical Algorithm for the Fractional Drinfeld–Sokolov–Wilson Equation. *Appl. Math. Comput.* **2018**, *335*, 12–24. [CrossRef]
28. Gao, W.; Veeresha, P.; Prakasha, D.G.; Baskonus, H.M.; Yel, G. A Powerful Approach for Fractional Drinfeld–Sokolov–Wilson Equation with Mittag-Leffler Law. *Alex. Eng. J.* **2019**, *58*, 1301–1311. [CrossRef]
29. Arafa, A.; Hagag, A. A New Semi-Analytic Solution of Fractional Sixth Order Drinfeld–Sokolov–Satsuma–Hirota Equation. *Numer. Methods Partial. Differ. Equ.* **2022**, *38*, 372. [CrossRef]
30. Arafa, A.; Hagag, A. Approximate Solutions for Some Reaction–Diffusion Systems with Non Integer Order. *Int. J. Appl. Comput. Math.* **2021**, *7*, 25. [CrossRef]
31. Liao, S. Homotopy Analysis Method: A New Analytical Technique for Nonlinear Problems. *Commun. Nonlinear Sci. Numer. Simul.* **1997**, *2*, 95–100. [CrossRef]
32. Jaradat, H.M.; Al-Shara, S.; Khan, Q.J.A.; Alquran, M.; Al-Khaled, K. Analytical Solution of Time-Fractional Drinfeld–Sokolov–Wilson System Using Residual Power Series Method. *IAENG Int. J. Appl. Math.* **2016**, *46*, 64–70.
33. Sahoo, S.; Saha Ray, S. New Double-Periodic Solutions of Fractional Drinfeld–Sokolov–Wilson Equation in Shallow Water Waves. *Nonlinear Dyn.* **2017**, *88*, 1869–1882. [CrossRef]
34. Ganie, A.H.; Yasmin, H.; Alderremy, A.A.; Shah, R.; Aly, S. An Efficient Semi-Analytical Techniques for the Fractional-Order System of Drinfeld–Sokolov–Wilson Equation. *Phys. Scr.* **2024**, *99*, 015253. [CrossRef]
35. Srivastava, H.M.; Baleanu, D.; Machado, J.A.T.; Osman, M.S.; Rezazadeh, H.; Arshed, S.; Günerhan, H. Some New and Modified Fractional Analysis of the Time-Fractional Drinfeld–Sokolov–Wilson System. *Chaos Interdiscip. J. Nonlinear Sci.* **2020**, *30*, 113104. [CrossRef] [PubMed]
36. Zhang, X.Z.; Asjad, M.I.; Faridi, W.A.; Jhangeer, A.; Inc, M. The Comparative Report on Dynamical Analysis about Fractional Nonlinear Drinfeld–Sokolov–Wilson System. *Fractals* **2022**, *30*, 2240138. [CrossRef]
37. Saifullah, S.; Ali, A.; Shah, K.; Promsakon, C. Investigation of Fractal Fractional Nonlinear Drinfeld–Sokolov–Wilson System with Non-Singular Operators. *Results Phys.* **2022**, *33*, 105145. [CrossRef]
38. Almetwally, E.M.; Zayed, M.A.; Mohamed, M.; Ragb, O.; Khidr, M.F.; Matbuly, M.; Salah, M. Numerical quadrature solution of fractional non-linear Drinfeld-Sokolov-Wilson system. *Bound. Value Probl.* **2026**, *2026*, 123. [CrossRef]
39. Alaroud, M.; Aldosari, F. Effective Analytical-Approximate Technique for Caputo Nonlinear Time-Fractional Systems Emerging in Shallow Water Waves and Hydrodynamic Turbulence. *Eur. J. Pure Appl. Math.* **2025**, *18*, 5784. [CrossRef]
40. Alqahtani, Z.; Hagag, A. A New Semi-Analytical Solution of Compound KdV–Burgers Equation of Fractional Order. *Rev. Int. Métodos Numéricos Cálculo Diseño Ingeniería* **2023**, *39*, 38. [CrossRef]
41. Arafa, A.A.M.; Hagag, A.M.S. A Different Approach for Study Some Fractional Evolution Equations. *Anal. Math. Phys.* **2021**, *11*, 162. [CrossRef]
42. Hussain, S.; Arora, G.; Kumar, R. Semi-Analytical Methods for Solving Non-Linear Differential Equations: A Review. *J. Math. Anal. Appl.* **2024**, *531*, 127821. [CrossRef]
43. Noor, S.; Alshehry, A.S.; Dutt, H.M.; Nazir, R.; Khan, A.; Shah, R. Investigating the Dynamics of Time-Fractional Drinfeld–Sokolov–Wilson System through Analytical Solutions. *Symmetry* **2023**, *15*, 703. [CrossRef]
44. Aboodh, K.S. The New Integral Transform "Aboodh Transform". *Glob. J. Pure Appl. Math.* **2013**, *9*, 35–43.
45. Cherif, M.H.; Ziane, D. A New Numerical Technique for Solving Systems of Nonlinear Fractional Partial Differential Equations. *Int. J. Anal. Appl.* **2017**, *15*, 188–197. [CrossRef]

46. Alfaqeih, S.; Ozis, T. Note on triple Aboodh transform and its application. *Int. J. Eng. Inf. Syst. (IJEAIS)* **2019**, *3*, 41–50.
47. Temimi, H.; Ansari, A.R. A Semi-Analytical Iterative Technique for Solving Nonlinear Problems. *Comput. Math. Appl.* **2011**, *61*, 203–210. [CrossRef]
48. Temimi, H.; Ansari, A.R. A Computational Iterative Method for Solving Nonlinear Ordinary Differential Equations. *LMS J. Comput. Math.* **2015**, *18*, 730–753. [CrossRef]
49. Arafa, A.A.M.; El-Sayed, A.M.A.; Hagag, A.M.S. A Fractional Temimi–Ansari Method (FTAM) with Convergence Analysis for Solving Physical Equations. *Math. Methods Appl. Sci.* **2021**, *44*, 6612–6629. [CrossRef]
50. Sultana, M.; Waqar, M.; Ali, A.H.; Alb Lupaş, A.; Ghanim, F.; Abduljabbar, Z.A. Numerical Investigation of Systems of Fractional Partial Differential Equations by New Transform Iterative Technique. *AIMS Math.* **2024**, *9*, 26649–26670. [CrossRef]
51. Almuneef, A.; Alqahtani, Z.; Abu Arqub, O.; Hagag, A. Convergence Analysis and Analytical Approximation of Fractional Modified Camassa–Holm and Degasperis–Procesi Equations via a Hybrid Transform–Iterative Framework. *Int. J. Mod. Phys. C* **2026**, 2750140. [CrossRef]
52. Christov, O.; Hakkaev, S.; Oh, S.; Stefanov, A.G. Dynamics of the Drinfeld–Sokolov–Wilson System: Well-Posedness and (in)stability of the Traveling Waves. *J. Differ. Equ.* **2025**, *439*, 113410. [CrossRef]
53. Zhou, Y.; Peng, L. On the Time-Fractional Navier–Stokes Equations. *Comput. Math. Appl.* **2017**, *73*, 874–891. [CrossRef]
54. Diethelm, K. *The Analysis of Fractional Differential Equations; Lecture Notes in Mathematics; Springer:* Berlin/Heidelberg, Germany, 2010.
55. Ye, H.; Gao, J.; Ding, Y. A generalized Gronwall inequality and its application to a fractional differential equation. *J. Math. Anal. Appl.* **2007**, *328*, 1075–1081. [CrossRef]
56. Jin, L.; Lu, J.F. Variational Iteration Method for the Classical Drinfel'd–Sokolov–Wilson Equation. *Therm. Sci.* **2014**, *18*, 1543–1546. [CrossRef]

Disclaimer/Publisher's Note: The statements, opinions and data contained in all publications are solely those of the individual author(s) and contributor(s) and not of MDPI and/or the editor(s). MDPI and/or the editor(s) disclaim responsibility for any injury to people or property resulting from any ideas, methods, instructions or products referred to in the content.